



FEDERAL UNIVERSITY OF SANTA CATARINA
TECHNOLOGY CENTER
CONTROL AND AUTOMATION ENGINEERING

Henrique Morales Busiquia

**Development of a Framework for Force Control in Laser Metal Deposition
Machines**

Florianópolis
2020

Henrique Morales Busiquia

**Development of a Framework for Force Control in Laser Metal Deposition
Machines**

Report was judged in the context of the discipline **DAS5511: Final Project Work** and **AP-PROVED** in its final form by the Control and Automation Engineering Course.

Advisor: Prof. Dr. Marcelo De Lellis Costa de Oliveira

Florianópolis
2020

Henrique Morales Busiquia

**Development of a Framework for Force Control in Laser Metal Deposition
Machines**

This monography was judged in the context of the discipline DAS5511: Final Work Project and approved on its final form by the following members of the examination board:

Jan Riepe, Dipl.-Ing.
Company Supervisor
Fraunhofer IPT

Prof.(a) Marcelo de Lellis Costa de Oliveira, Dr(a).
University Advisor
Federal University of Santa Catarina

Prof.(a) Gustavo Artur de Andrade, Dr(a).
Evaluator
Federal University of Santa Catarina

Igor De Oliveira Silvestre
Speaker
Federal University of Santa Catarina

Márcio Sumariva Nandi
Speaker
Federal University of Santa Catarina

ACKNOWLEDGEMENTS

As it always should be, first, I would like to thank my family for all support. To my parents, who gave me the possibility of always studying in good institutions. And for them, always supporting me to follow my regardless of where these goals were, despite them always wanting our distance to be closer. To my brother Douglas, who always give me good conversations when it was necessary.

To all my professors and supervisors during this graduation on Brazil, Canada and Germany who share their time and experience with me. In special, I would like to thank Prof. Marcelo Stemmer, who was my internship supervisor and the responsible for the program that made it possible to write this project in Germany. To Jan Riepe, who gave me the opportunity and the theme for working during my work. Also, to Prof. Marcelo De Lellis, who shared his time to advise me during this project.

To my Brazilian friends in Aachen, who made this one year abroad almost like home. In special, for Igor, who gave all the support while coming to Germany. For Ivan, Leonardo and Arthur, who were always a good company during this time. For Gabriel and Nivaldo, who were also good work colleagues giving the necessary assistance to this work.

To my friends in Brazil, that gave me the support during my graduation days. In special for my graduation classmates, who have always being good friends during the classes and exams. For Dimitri, who since our childhood shared with me good memories.

A special thanks to Helena, who was a great company during the development of this work despite all the difficulties.

RESUMO

A busca pela otimização na utilização de recursos, nos métodos de processo e por alternativas mais rentáveis ocasiona a necessidade de a indústria estar sempre investindo em alternativas para soluções já presentes no mercado. Recentemente, houve um rápido aumento no interesse pela área de manufatura aditiva. Dentro das alternativas estabelecidas para esta área, encontra-se a deposição de metal por laser. Nesta técnica, cria-se um banho de fusão no componente no qual o metal é aplicado continuamente e assim derretido. Este metal pode ser aplicado em forma de pó ou na forma de arame. Devido a vantagens técnicas oferecidas pela deposição por arame, este trabalho abordará o estudo de uma técnica para tornar este processo mais estável. Utilizando as forças entre o arame e a camada depositada, um controle em malha fechada é aplicado ao processo. Para isso, a posição da ferramenta de deposição é utilizada como variável de controle. Ainda, duas formas de utilizar as forças são estudadas. Além do mais, a indústria tem feitos grandes investimento na área de *big data*. Devido à facilidade em aquisição e armazenamento de grandes volumes de dados, um grande esforço para criação de grandes bancos de dados sobre processos industriais está sendo realizado. Para isso, neste trabalho, um banco de dados não relacional para coletar as informações durante as deposições foi gerado. Ferramentas para pré-processamento destes dados antes de serem armazenados, visualização e análise dos mesmo foram desenvolvidas. Por fim, utilizando estas informações, a identificação do sistema para controle foi realizada.

Palavras-chave: Manufatura aditiva, Deposição de metais a laser, Indústria 4.0 ,Sistemas de controle

ABSTRACT

The industry is always investing in research to find alternatives for optimizing the use of its resources, process methods and reach more profitable products. Recently, there has been a rapid increase in interest in the area of additive manufacturing. Laser metal deposition is among the alternatives being researched for this area. In this technique, a melt pool is created by a laser in the component in which the metal is continuously applied and melted. This metal can be added in powder or wire form. Due to the technical advantages offered by wire deposition (LMD-W), this work will approach the study of a technique to make LMD-W a more stable process. By using the measured force as the controlled variable, a position control is performed during the deposition. For that, the control action is applied to the height of the deposition tool. Also, two methods of using the force to regulate this process are studied. Furthermore, the industry has made great investments in the area of *big data*. Due to the current capacity of acquisition and storage of large volumes of data, a great effort is being made to create large databases on industrial processes. A non relational database was developed in this project for storing the information acquired during the deposition. Tools to process, visualize and analyze these data were developed during this work. In addition, this data is used for identifying the system model for controlling the process.

Keywords: Additive manufacturing, Laser metal deposition, Industry 4.0, Feedback control systems

LIST OF FIGURES

| | |
|--|----|
| Figure 1 – Sales of materials for polymer powder bed fusion were at an all-time high in 2018. | 12 |
| Figure 2 – Schematic of a LMD Process | 13 |
| Figure 3 – Fraunhofer Institute for Production Technology (IPT) Building | 14 |
| Figure 4 – Setup of Laser Metal Deposition using Coaxial Powder Nozzle | 19 |
| Figure 5 – Laser Metal Deposition using Wire as Material | 20 |
| Figure 6 – LMD Variables | 20 |
| Figure 7 – Possible cases where the distance affects the quality of the product | 22 |
| Figure 8 – Process Dynamic Evaluation through test signals | 24 |
| Figure 9 – Step test to identify first order transfer function | 25 |
| Figure 10 – Classic Closed Loop Model | 26 |
| Figure 11 – Position for Z-Axis in relation to X-Axis for five layers deposition | 29 |
| Figure 12 – Comparison between the dynamics through multiple layers | 30 |
| Figure 13 – A deviation propagating through layers | 31 |
| Figure 14 – Forces Reaction for third layer deposition | 32 |
| Figure 15 – Different dynamics observed on the edges of the bead | 32 |
| Figure 16 – Saturation tests during the deposition | 33 |
| Figure 17 – Table describing the hardware and software parameters used during the depositions of this project | 34 |
| Figure 18 – Measured Force-Axis in the deposition | 35 |
| Figure 19 – A- Ideal position of the deposition Tool; B- Deposition Tool requiring a correction | 35 |
| Figure 20 – Path from the data observed in the Process until saving in the cloud | 36 |
| Figure 21 – A vBox is seen on the left while the necessary communication card is presented on the right | 37 |
| Figure 22 – Acquisition Software Graphical User Interface (GUI) | 38 |
| Figure 23 – Acquisition Software Flow | 39 |
| Figure 24 – Unified Modeling Language (UML) Representation of MongoDB | 41 |
| Figure 25 – Four variables that can be monitored through the live dashboard | 42 |
| Figure 26 – Archive Data Datashboard | 43 |
| Figure 27 – Hardware Setup | 44 |
| Figure 28 – Datasheet Information from the Force Sensor | 45 |
| Figure 29 – Hardware used for transforming force into voltages | 45 |
| Figure 30 – Field Programmable Gate Array (FPGA) A- Acquisition Module; B- Control Module; C- Ethernet Communication | 46 |
| Figure 31 – Datasheet Information from the Acquisition Module | 46 |
| Figure 32 – Datasheet Information from the Control Module | 47 |

| | |
|---|----|
| Figure 33 – Data flow inside the Labview VI | 48 |
| Figure 34 – Data flow inside the Computer VI | 49 |
| Figure 35 – Laboratory Virtual Instrument Engineering Work-bench (LabVIEW) GUI | 50 |
| Figure 36 – The Computer Numeric Control (CNC) Panel and the processing head of the LMD setup | 51 |
| Figure 37 – Pseudocode from the G-Code used during the open loop depositions . | 51 |
| Figure 38 – Using matlab plot for defining the system parameters | 54 |
| Figure 39 – Unitary step response for equation Equation (20) | 55 |
| Figure 40 – Simulated and real step response | 56 |
| Figure 41 – Graphs Displaying the position and the force in three layers | 57 |
| Figure 42 – Acquired data used for identifying a first order function | 58 |
| Figure 43 – Multiple Plots from different transfer functions to this system | 59 |
| Figure 44 – Step result in the second layer for a perturbation in the Z axis | 60 |
| Figure 45 – Comparison between the step using the real data and the model . . | 61 |
| Figure 46 – Multiple Plots from different transfer functions to this system | 61 |
| Figure 47 – Problems caused by an abrupt change in the control signal | 62 |
| Figure 48 – Using the Sisotool toolbox for tuning the control parameters | 64 |
| Figure 49 – Force in the second layer | 65 |
| Figure 50 – Melt Pool Positioning | 66 |
| Figure 51 – Comparison between the control action in the four tests | 67 |
| Figure 52 – Results for both Z-Control in the sixth layer | 68 |
| Figure 53 – Measured Forces in relation to the position in the deposition of all layers using the control C_{z_1} with a default offset | 69 |
| Figure 54 – Control action in the deposition of all layers using the Control C_{z_1} . . | 69 |
| Figure 55 – Resultant Bead using the control C_{z_1} | 70 |

LIST OF ABBREVIATIONS AND ACRONYMS

| | |
|---------|--|
| AM | Additive Manufacturing |
| CNC | Computer Numeric Control |
| DAQ | Data Acquisition |
| FPGA | Field Programmable Gate Array |
| GUI | Graphical User Interface |
| IPT | Institute for Production Technology |
| JSON | JavaScript Object Notation |
| LabVIEW | Laboratory Virtual Instrument Engineering Work-bench |
| LMD | Laser Metal Deposition |
| LMD-P | Laser Metal Deposition with Powder |
| LMD-W | Laser Metal Deposition with Wire |
| MIMO | Multiple Input - Multiple Output |
| NI | National Instruments |
| PC | Personal Computer |
| PI | Proportional integral |
| SISO | Single Input - Single Output |
| SL | Stereolithography |
| SLS | Selective Laser Sintering |
| UML | Unified Modeling Language |
| VI | Virtual Instrument |

LIST OF SYMBOLS

| | |
|-----------------|---|
| C_{z_1} | Control Transfer Function using the First Order Model of Z-Force |
| Δm | Mass change |
| τ | Time Constant |
| K_g | Static gain of the Model |
| θ | Time Delay |
| K_p | Proportional Gain |
| K_i | Integral Gain |
| ζ | Damping Ratio |
| ω_n | Natural Frequency |
| T_s | Settling Time Second Order System |
| z_{dt} | Z position of the Deposition Tool |
| x_{dt} | X position of the Deposition Tool |
| y_{dt} | Y position of the Deposition Tool |
| Δz_{dt} | Change of Deposition Tool Position |
| h_{layer} | Height Layer |
| F_{res} | Resultant Force |
| F_x | Force in X-Axis |
| F_y | Force in Y-Axis |
| F_z | Force in Z-Axis |
| t | Time |
| C_{z_2} | Control Transfer Function using the Second Order Model of Z-Force |
| C_{res_1} | Control Transfer Function using the First Order Model of Resultant Force |
| C_{res_2} | Control Transfer Function using the Second Order Model of Resultant Force |

CONTENTS

| | | |
|--------------|---|-----------|
| 1 | INTRODUCTION | 11 |
| 1.1 | ADDITIVE MANUFACTURING | 11 |
| 1.2 | FRAUNHOFER IPT AND THE RESEARCH INFRASTRUCTURE . . . | 14 |
| 1.3 | GOALS AND METHODOLOGY | 15 |
| 1.4 | CORRELATION WITH THE CONTROL AND AUTOMATION ENGI- NEERING COURSE | 17 |
| 2 | TOOLS AND METHODS | 18 |
| 2.1 | LASER METAL DEPOSITION | 18 |
| 2.1.1 | Laser Metal Deposition with Powder | 18 |
| 2.1.2 | Laser Metal Deposition with Wire | 19 |
| 2.2 | BIG DATA | 22 |
| 2.3 | CONTROL THEORY | 24 |
| 2.4 | SOFTWARES | 27 |
| 3 | PROBLEM DEFINITION | 29 |
| 4 | FRAMEWORK DEVELOPMENT | 36 |
| 4.1 | DATA ACQUISITION | 37 |
| 4.1.1 | Hardware | 37 |
| 4.1.2 | Acquisition Software | 38 |
| 4.2 | MACHINE COMMUNICATION | 43 |
| 4.2.1 | Instrumentation and Signal Processing | 43 |
| 4.2.2 | Labview Program | 46 |
| 4.2.3 | CNC | 50 |
| 4.2.4 | G Code | 50 |
| 5 | FORCE CONTROL | 53 |
| 5.1 | SYSTEM IDENTIFICATION | 53 |
| 5.2 | CONTROL DESIGN | 59 |
| 6 | CONCLUSION AND OUTLOOK | 71 |
| | REFERENCES | 74 |

1 INTRODUCTION

In this chapter, the concepts used during this project are presented. The first section presents an introduction to the area of additive manufacturing. Afterwards, the institute where this work was developed is presented. In the end, the methodology and goals to achieve during the project and its correlation with the Control and Automation Engineering Course are presented.

1.1 ADDITIVE MANUFACTURING

Additive Manufacturing processes, also known as generative manufacturing, are all manufacturing processes that joins materials, preferably in a layer by layer method, for creating a piece, while being supervised by a computer as defined by Gebhardt (2013).

Comparing to traditional manufacturing technology, Lu, Li, and Tian (2015) define Additive Manufacturing (AM) as the process which the mass change of the part is positive $\Delta m > 0$. In contrast, the part mass decreases during the subtractive manufacturing process.

3D Printing, another term for this process, resembles biological processes by creating products layer-by-layer. This method offers an advantage from traditional subtractive methods for producing less waste of material. Besides the economical benefit of decreasing the volume of material spent, Gebler, Schoot Uiterkamp, and Visser (2014) also indicates AM as a more sustainable option as it can reduce the environment impact of the business.

This is one of the reasons that inventions and creations in 3D printing are becoming more and more prevalent. Despite the fact that this process is relatively new, the first prototype of a stereolithography machine was developed in 1986 by Chuck Hull as described by Printing)" (2014). Lu, Li, and Tian (2015) says its potential is already impacting traditional processes as the machining, that emerged more than 300 years ago.

One year later from its first prototype, 3D Systems, a company also owned by Chuck Hull, developed the first commercially available AM machine in the world. Using a laser, Stereolithography (SL) solidified thin layers of ultraviolet (UV) light-sensitive liquid polymer.

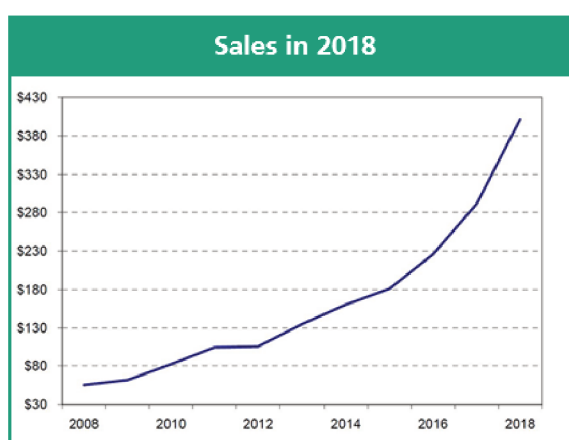
In 1992, Selective Laser Sintering (SLS) 3D Printing were made available by the company DTM. This technology was developed during the same time as SL as outlined by Wong and Hernandez (2012). SLS also uses laser as the Power source, yet, it uses powdered material for creating the solid structure by sinterization. This company was later acquired by 3D Systems.

These two are examples of the first AM technologies developed during the 1980s.

Regardless of its first application being made available on this decade, the first researches on this topic were made in the 1960s and in the 1970s. Nonetheless, the two first decades of the 2000s were the period of real growth for AM.

In the last 5 years, Association (2018) shows that the revenue from metals grew an estimated 41.9%. This development can be verified on Figure 1 in a million of dollars and it can be linked to the increase in use of Metal in Addictive Manufacturing. Furthermore, the AM industry saw a 21% growth in revenue on the year of 2018.

Figure 1 – Sales of materials for polymer powder bed fusion were at an all-time high in 2018.



Source: Association (2018)

Cooper (2001) indicates that the quick advance in the studies in 3D objects printing were possible through the development made in computer aided design (CAD), manufacturing (CAM), and computer numerical control (CNC). Also, Cooper (2001) indicates the influence of the spread in low cost computers on this factor, inclusively, reflecting in the desktop 3D printers industry.

After its popularity increase, the use of the 3D printer term is usually correlated with Fused filament fabrication (FFF) devices. Hairul Hisham Hamzah et al. (2018) define this as a 3D printing process that heats a continuous filament of a thermoplastic material through an extrusion head, and, after that, it deposits on the growing work. The use of this process for hobbyist-grade 3D printing, especially for its low cost, made this one of the famous rapid prototyping process.

Hagqvist, Christiansson, and Heralic (2015) cites flexibility as one of the main reasons of the additive manufacturing adoption. As a flexible process, this can be used for producing desk lamps at home by a low-cost printer, but also for repairing turbo-engine components. This flexibility also brings benefits when a level of customization is necessary during the fabrication. For example, Lu, Li, and Tian (2015) cites this benefit when producing artificial implants and medical rehabilitation equipment and devices.

Another reason for applying generative manufacturing instead of the traditional methods is its design freedom. Using additive techniques, several parts made of the various material can be replaced by one integrated assembly. Furthermore, by adding the material on a layer-to-layer method, complex geometries can also be achieved more easily due the lack of limitations existing in the subtractive process as risk of collision, diverse tooling and need for fixtures.

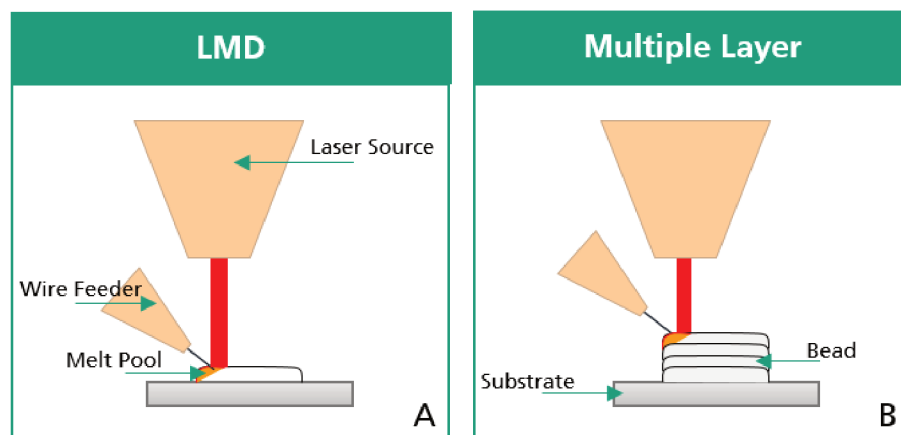
In order to meet the demands from high-end industries, and by exploring this advantage of the process, the recent focus of AM research has shifted to fabricate complex-shaped metal components, including titanium and nickel. This free-form fabrication of metallic objects has produced many methodologies for production, such as Direct Metal Laser Sintering (DMLS), Laser Metal Deposition (Laser Metal Deposition (LMD)) and Electron-Beam melting (EBM).

According to Gao et al. (2015), the rapid proliferation of AM technologies is driven by the increase in the variety of materials, low-cost machines, and potential for new application areas

Depending on the energy source used for metal deposition, wire-feed AM can be classified into three groups, namely: laser based, arc welding-based and electron beam-based. Laser has been the most popular between them due to its precision.

In the Figure 2, the process studied in this work is illustrated. First, a laser source is used for heating a substrate and in consequence creating a melt pool. Afterwards, a wire feeder is used for applying metal into this process. By melting this material while the deposition tool travels in the direction of the wire feeder, a new layer is created. In the end, a bead is produced after adding a layer on top of each previous layer.

Figure 2 – Schematic of a LMD Process



Source: Original

1.2 FRAUNHOFER IPT AND THE RESEARCH INFRASTRUCTURE

The IPT is an institution of the Fraunhofer-Company for the Promotion of Applied Science. This branch, seen on Figure 3, develops technologies and advises companies on the optimization of their products, production process and services.

The Fraunhofer-Company has over 26000 employees working in more than 80 research institutes throughout Germany. It was created in 1949 aiming to carry out application-oriented research for direct benefit to companies. Its budget of over 2.0 billion euros are used in many fields of society, for example, in the same city as IPT, there are research centers for Molecular Biology and also for Laser Technology.

Figure 3 – Fraunhofer IPT Building



Source: (FRAUNHOFER. . . , 2020)

Located on the grounds of Rhine Westphalia Technical University (RWTH) in Aachen, the focus of IPT is developing solutions for manufacturing companies. The areas of process technology, production machines, mechatronics, production quality and metrology as well as technology management are between the main focus of this research center.

Between these topics, one department is for studying the non-conventional manufacturing processes and technology integration. This includes additive manufacture, laser technologies such as laser deposition welding, laser hardening and laser structuring, among others solutions. Headed by Dr.-Ing. Kristian Arntz, the goal of this department is to develop non-conventional alternatives and integrates them into existing processes.

This project is developed in the group of laser materials processing. Under the leadership of Dipl.-Ing. Jan Riepe, different industrial solutions using laser as the energy source are studied by this team. For example, the solutions can be focused on treating surfaces, looking to attend the today's market requirement of designing components with sufficiently stress-resistant subsurface areas, through laser hardening.

Other technique studied in this division is the laser structuring of geometrically complex components with short-pulse and ultra-short pulse lasers. Known as Laser Ablation, one of its advantage is the highly flexible functionalization of surfaces with nano- and microstructures.

Also, with the supervision of Dipl. -Ing. Jan Riepe, one of the group applications is Laser Metal Deposition. As covered on the next chapter, this process has many uses as for different tools modification and repair, and also for building complex and structural components.

One of the products of the laser materials processing is the LMD-W-20-L. This module for wire deposition welding was projected for easily integrated within existing process chains, handling systems or machine tools. Also using wire as material for the laser deposition, Alzmetall is the machine used during this project. By integrating an optical laser spindle into a 5-axis milling machine, this setup offers also an alternative for laser surface treatment.

1.3 GOALS AND METHODOLOGY

The main goal of this project is the development of a first framework for creating a force control for Laser Metal Deposition with Wire (LMD-W). By developing a framework for this system, all the tools necessary for acquiring information, visualizing it and regulating the force during the deposition are developed.

Using a Single Input - Single Output (SISO) control, two variables are directly used in this project. The Force between the wire and the bead is the controlled variable. This variable should follow a certain reference defined by the user. The distance between the laser beam and the substrate in the Z-direction is manipulated for reaching this goal. This closed loop is reached by implementing several sub-projects.

First, a database is implemented where all the interest parameters involved in the process are stored. This database will be populated using data of sensors, actuators and user preferences. These values are acquired by open loop tests initially. For processing and storing this data, a software is developed.

After evaluating these open loop values, a first control approach is defined for creating a closed loop Proportional integral (PI) control. In this PI, the position of the processing head to the substrate material will be defined as the controller output. For calculating the control action and communicating to the CNC, another program is developed. Also, the G-Code necessary for reading the input to the deposition tool is

developed. For evaluating this method in real time, live dashboards will be created for displaying the current process state.

The methodology established to reach the project goal consists of the following main steps:

1. Development of a middleware that acquires signals from sensors and actuators and saves to a database:
 - a) Acquiring Signals from sensors, processing and converting them to the database format using C#;
 - b) Define communication with a MongoDB server.
2. Development of real time dashboards for real time process monitoring:
 - a) Communication with MongoDB to extract data;
 - b) Development and deployment of web dashboards using HTML, JS and CSS.
3. Programs for closing the loop with the CNC
 - a) Labview program for selecting how the input to the CNC is defined;
 - b) G-code for reading and inserting the LabVIEW input into the process
4. Open loop tests to populate the database:
 - a) Defining interest parameters to execute step tests;
 - b) Generating G code for executing the process.
 - c) Studying the effects of the parameters of the process in the measured force
5. Development and testing of a first force control method:
 - a) Cleaning the data in Jupyter notebook to identify the system
 - b) Using Matlab toolbox for proposing four models to the system based in two variables: Resultant Force or Z-Force
 - c) Tuning the control parameters.
 - d) Applying the control in the G-Code
6. Result Analysis:
 - a) Comparing the performance of both variable studied.
 - b) Evaluating the benefit on process by comparing process results with and without force control applied.

1.4 CORRELATION WITH THE CONTROL AND AUTOMATION ENGINEERING COURSE

The control and automation course is focused in three major areas: Process Control; Industry Computing; Manufacturing Automation. Despite this work being focused on the development of a control, therefore, its major focus will be on this area, the other fields are also going to impact during at least one phase of the project.

The first area used will be industrial computing. During the five-year-long course, the control and automation student develops a strong background in different programming languages. This also will be used for implementing a digital controller, presented in different semesters of the formal curriculum of this undergraduate course. Moreover, all the data acquired during the process will be dealt using a database and it is expected to be the source of algorithms to identify this system's dynamic.

Also, the CNC coding knowledge provided by disciplines in Manufacturing Automation will be necessary as the current machine is controlled by G-Code. Additionally, the current problem requires an operator to manipulate the desired position of the laser in the process. This solution will replace this need, making the operator able to focus other tasks that influence in the final piece quality.

Ultimately, as mentioned this project main focused is to offer a control solution to this process. Thus, many topics of this field will be indispensable on the progress of this work. In special, the need for identifying the system dynamics, a required step to develop a model based control.

2 TOOLS AND METHODS

In this chapter, the area of production where this project is being developed is presented. First, the LMD process is introduced. A comparison between the process using wire and using powder as material is made by exposing in which area they are more applicable, their advantages and limitations. Also, big data terms used by this project are presented. At the end, the control and tools used during this project are discussed.

2.1 LASER METAL DEPOSITION

Stefan Kaielerle et al. (2012) describes powder and wire as the most common technologies used for laser deposition. As this project works with LMD-W, only a brief description for Laser Metal Deposition with Powder (LMD-P) and its differences for the process made by wire will be presented before moving the focus to the main process.

2.1.1 Laser Metal Deposition with Powder

Using the same energy source, the difference in the production of the part during this process is the material. By selecting a powdered material for manufacturing, it also creates the possibility of a different machine design.

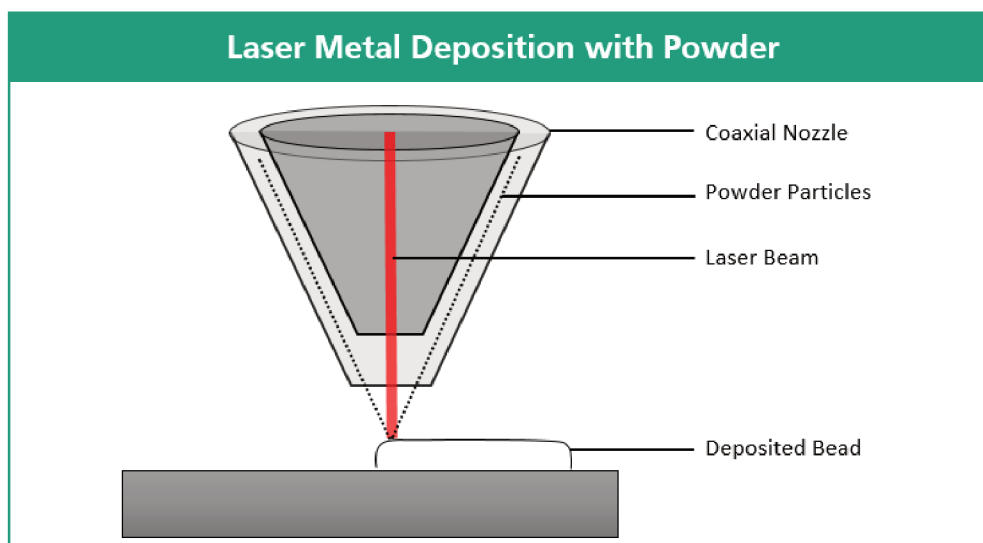
While the LMD-W only can be achieved through a lateral nozzle feeding the wire, the LMD-P can be achieved using this construction, but also, the powder deposition can use a coaxial powder nozzle, as observed in Figure 4. In contrast to the present setup, that only uses powder, this process can also be combined with a wire feeder.

When using only powder, the process starts by creating a melt pool by heating the part up using a laser beam. At the same instant, powder is introduced to the melt pool by the nozzle combining with the base material to form a new layer. Several layers can be combined to increase the total height of the object, as each new layer has between 0.3mm and 2mm depending on the chosen parameters as cited by K. Löffler (2013)

Its material high cost and the possibility of the operator developing health issues due the powder toxicity can be one of the disadvantages that choosing this material creates. In addition to the price of the usual used powder components, Mahamood et al. (2013) indicates that this process does not offer a high efficiency deposition, leading to the necessity of studies to take advantage of the unused material.

On the other hand, the powder-based LMD produces a very stable process, creating an advantage in comparison with its wired-based alternative. Brueckner et al. (2017) cites the absence of problem in the contact between the melt pool and the material being fed to the produced part as one of the reasons that this option offers

Figure 4 – Setup of Laser Metal Deposition using Coaxial Powder Nozzle



Source: Original

more stability. This is used for producing complex geometries, another advantage that this process offers.

2.1.2 Laser Metal Deposition with Wire

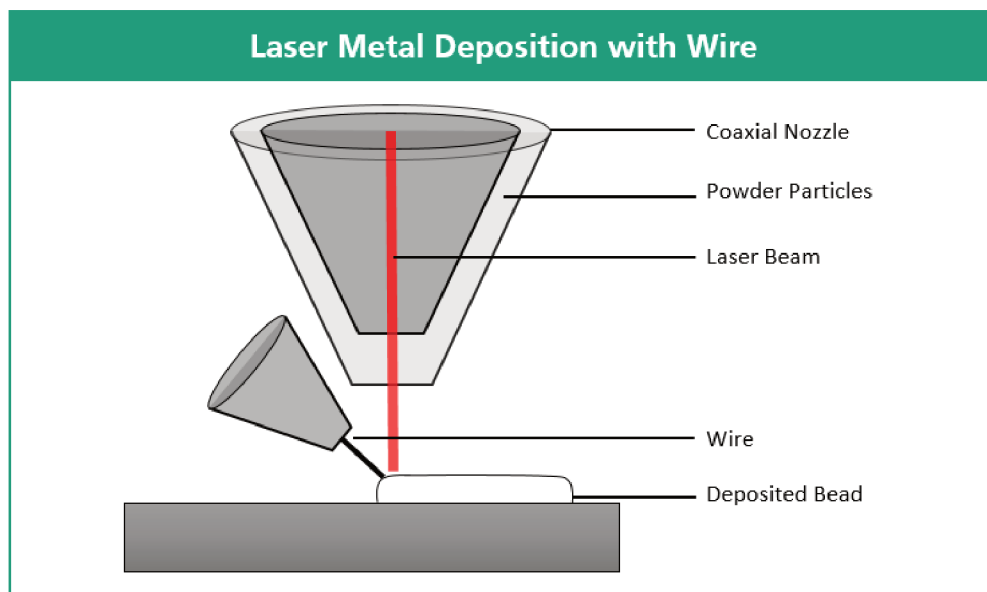
Additionally to powders, the chosen metal can also be added to the process using a wire feeder. In the Figure 5, a lateral wire-feeder adding the material to the melt pool can be observed. This is the general approach used for wire systems, but coaxial wire nozzle has also already studied as shown by Association (2018).

This schematic is usually used positioning the wire at the leading edge of the melt pool. By using this to define the process direction, moving in the left direction on the Figure 5 for example, the system was proved to be more stable. This is one of the various parameters known to influence the final result of the manufactured part.

Due this large number of variables that are involved in the process, it is critical to detect the cause of a process failure that may compromise the final result of a part to guarantee robustness to the system. Nonetheless, the study of these influences is still on an initial stage, as it is still not clear how each variable specifically affects the desired outcome. Even more, an eventual failure can be the result of multiple causes.

In the Figure 6, a distinction between the involved variables are presented. It can be easily observed some variables that both processes shares that affects the part manufacturing. An example is Laser Power that directly affects how the state of the melt pool is when the material is injected for manufacturing a new layer. Studies have been made by Mahamood et al. (2013) examining this variable effect on the quality of the

Figure 5 – Laser Metal Deposition using Wire as Material



Source: Original.

final piece.

Figure 6 – LMD Variables

| Actuating Variables | Control Variables |
|---|--|
| <ul style="list-style-type: none"> ■ Laser power ■ Feed rate ■ Wire feed rate ■ Shielding gas flow rate ■ Focal position ■ Focal spot geometry ■ Toolpath <ul style="list-style-type: none"> – Stepor distance – Operating angles – Layer Height | <ul style="list-style-type: none"> ■ Topography ■ Position ■ Temperature ■ Melting Pool Size ■ Force (Wire contact) |

Source: IPT 130 Department

The interaction between the substrate and the laser creates the melt pool. As a conclusion, the relationship among this actuating variable and one control variable can be clearly recognized. By using a coaxial camera, the change in its size can be monitored, thus, J.T. Hofman et al. (2012) proposed using these two variables in closed-

loop control.

Other relations can be obtained involving the laser power. A closed-loop control for the width of the produced bead was already developed by Almir Heralić, Anna-Karin Christiansson, Kjell Hurtig, et al. (2008) based on an approximately linear correlation between this actuating variable and the width on the bead produced.

The search for making the wired-based process to reach the powder-based stability state increases based on its advantages offered compared to its equivalent. The use of wire offers a better efficiency of material usage, where it can reach almost 0% of material waste.

This better performance also reflects in other enhancements as in higher deposition rates, where the powder-based technologies can reach only $10g/min$, while its peer can reach $330g/min$ as discussed by Ding et al. (2015). This allows for the economical production of larger geometries with moderate complexity.

Adding to a better work environment, due the decrease in health problems to the operators, and the economic advantage offered, due the low costs of the material and higher efficiency, there are also studies presenting the evidence of a better result in metallography analysis.

By studying the material properties of parts produced by both wired- and powder-based processes, Waheed Ul Haq Syed and Lin Li (2005) concludes that micro-structures from these different materials are similar, however more porosity is found in the powder-fed deposited parts. In the macroscopic side, wire-based techniques gives better surface finish, making it also more suitable to use for large structures with moderate complexity.

These benefits encourage the research for making LMD-W as stable as the LMD-P, making it a more complete solution. The difficulty in developing an appropriate instrumentation for online monitoring concomitantly with the short knowledge of the full effect of variables in this process dynamics can be noted as reasons for the slow advancement on that regard.

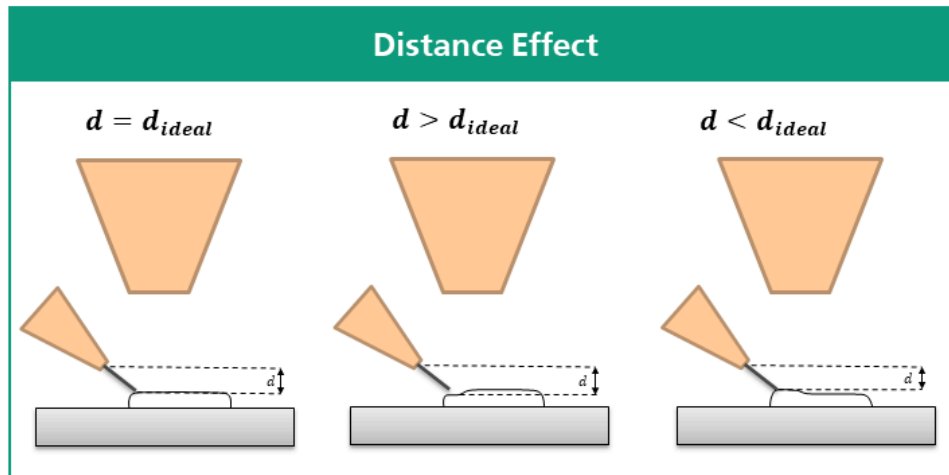
As an alternative for online measurement, Almir Heralić, Anna-Karin Christiansson, Mattias Ottosson, et al. (2010) has used post-process evaluation for increasing the quality of the final part. This alternative is efficient specially for the bead height, as the monitoring of this variable during the deposition is really challenging due to the high brightness of the molten metal.

A layer-to-layer control is applied using this technique. One method is using a 3D camera to inspect the height of the layer, while calculating the deviation on the reference, for correcting this error on the next layer. By repeating this process for building higher parts, Almir Heralić, Anna-Karin Christiansson, Mattias Ottosson, et al. (2010) integrates an iterative learning control algorithm for regulating this variable.

Haggqvist, Heralić, et al. (2015) cites the definition of an optimal distance between

the wire feeder and the bead a common problem during the LMD-W process. If the distance is too high, there is a weak link between the material and the bead resulting in a droplet as in the middle representation of the Figure 7.

Figure 7 – Possible cases where the distance affects the quality of the product



Source: Original

Also, as the right representation of the Figure 7 shows, if the distance is too low, the wire can bend through the weld pool. This leads to lack-of-fusion defects in the deposited material. On the left side of the Figure 7, an ideal case is shown, where the ideal distance ideal is kept through the deposition resulting in good beads.

2.2 BIG DATA

Big data is a term which describes large volume of diverse, complex and fast-changing data, derived from various sources. According to Gantz J (2011), in 2011, the overall created and copied data volume in the world was 1.8ZB ($\approx 1021B$), which increased by nearly nine times within five years.

This rapid increase in data production, powered by technological advances, which provide transformation in many equipment as sensors, machines and IT systems. This transformation allowed the connection of all this equipment along the value chain beyond a single enterprise. These connected system, interacting with each other, analyzing data to predict failure and adapting to changes in the process is the goal of the industry 4.0.

Also called fourth industry revolution, industry 4.0 is the trend towards automation and data exchange in manufacturing technologies and processes which include cyber-physical systems (CPS), the internet of things (IoT) and artificial intelligence. In this

context, the collection and comprehensive evaluation of data from many sources will become standard to support real-time decision-making.

2.2.1 Database

For organizing this vast volume of data flow, a database is used for collecting the information and storing on a cloud or in a local computer. The management of a database system can be divided according to the models that they support. Relational database organizes data into tables. These tables can be linked into each other, allowing the user to create an entirely new table from data in one or more tables.

Non relational database are not constructed using tables. Instead, they are called document-oriented. This document allows multiple categories of data to be stored in one entry. Thus, describing an online store system, instead of constructing two tables, one for storing all their customers and another for storing each order, this document can store the information from a single client and respectively have a subcategory with his orders.

MongoDB

MongoDB is a cross-platform document-oriented database program. Classified as a NoSQL database program, MongoDB uses JSON-like documents with schema. By using this type of document, this software allows easy integration between multiple stages of this program. JSON allows an integration with *C#* used by the software developed for acquiring the data and by ASP.NET, for retrieving the data to the dashboard. Also, python can easily manipulate this type of data.

2.2.2 Data Science

Data science is the area of study that combines programming skills, and knowledge of mathematics and statistics to extract meaningful insights from large amount of data. There are multiple steps inside a data science project until reaching a model to apply machine learning algorithms to it. In this project, three areas of data science are used:

- Data Collection: Using MongoDB to store the collected data in a document-oriented platform;
- Data Processing: Using *C#* to pre-process the data and transform in the MongoDB format and also by python and ASP.Net for post-processing the data for the next step;

- Data Understanding: Using the ASP.Net for creating a dashboard where monitoring of the data during a test can be made and also for a first analysis of previous tests.

2.3 CONTROL THEORY

In this section, the steps necessary for identifying a transfer function, the parameters used and a closed loop transfer function are presented.

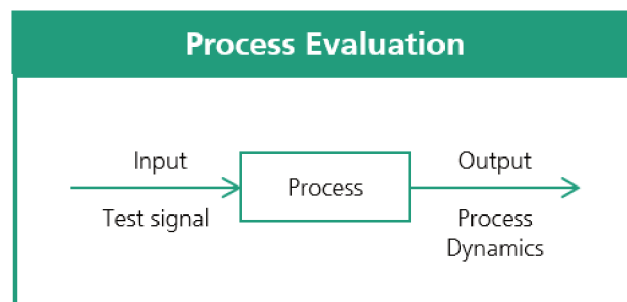
2.3.1 System Identification

First order models with a time delay are used in numerous different applications, where the main dynamic is reasonably damped as seen in (GENE F., J. DAVID POWELL, ABBAS EMAMI-NAEINI, 2010). This model needs 3 parameters: Time constant τ ; gain K_g and a time delay θ . They are used in the following 1st order transfer function:

$$G_p(s) = \frac{K_g}{\tau s + 1} e^{\theta s}. \quad (1)$$

These first order models are also the basic approach for a number of controller tuning methods, including the PI method. Nonetheless, before calculating this controller, it's necessary to define the values of these parameters. One of the most used methods for estimating these parameters in stable first order systems is to apply an open loop test on it. This test is represented in the Figure 8.

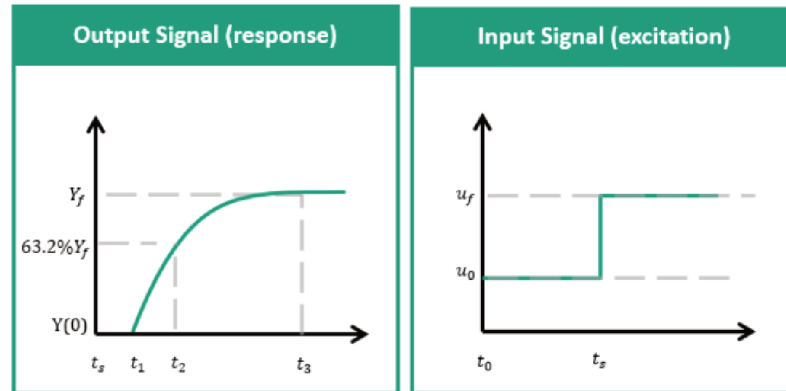
Figure 8 – Process Dynamic Evaluation through test signals



Source: Augusto Rodrigues Coelho, Antonio and dos Santos Coelho, Leandro (2016)

The common signals used as an input during the tests are: impulse, step, ramp and sinus. Augusto Rodrigues Coelho, Antonio and dos Santos Coelho, Leandro (2016) cites step response as one of the most used for this test. This signal, seen in the Figure 9, is obtained through the increment or decrement in the amplitude of the control variable signal of the system.

Figure 9 – Step test to identify first order transfer function



Source: Augusto Rodrigues Coelho, Antonio and dos Santos Coelho, Leandro (2016)

From the response observed in the Figure 9, the gain K_g of the system can be obtained by the following equation:

$$K_g = \frac{\Delta Y}{\Delta u} = \frac{Y_f - Y(0)}{u_f - u(0)}. \quad (2)$$

There are many methods to calculate the time constant τ of the system. From the Hägglund method, the time constant τ can be calculated when the response curve reaches the value $Y(t) = Y(0) + 0.63 Y_f$, following the equation:

$$\tau = t_2 - t_1 \quad (3)$$

where t_2 and t_1 can also be observed in the Figure 9. At the end, from the same signal, the delay of the response θ can also be calculated following:

$$\theta = t_1 - t_0. \quad (4)$$

2.3.2 Closed Loop

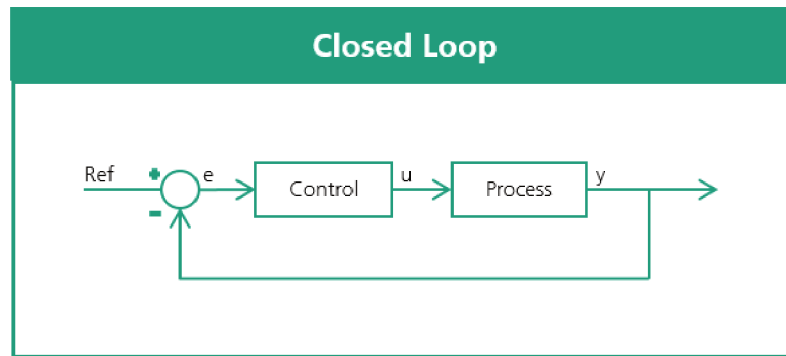
In a closed loop control, a controller is responsible for sending the input signal for the process. This signal is calculated by the controller observing the current error of the process. This system can be observed in the Figure 10.

Using a PI Controller, its signal is calculated by the current state of the error and its integral, as the following equation:

$$u(t) = K_p e(t) + K_i \int_0^t e(\tau) d\tau. \quad (5)$$

As defined by Edwards and Postlethwaite (1998), if an error is large enough and/or persists long enough, it is mathematically possible for the integral term to grow

Figure 10 – Classic Closed Loop Model



Source: Ogata (2016)

very large. This large input combined with the other elements of the equation can lead to a saturation in the control signal.

After applying the Laplace transformation on the controller equation, Ogata (2016) shows that the transfer function of this system is represented by:

$$C(s) = K_p + \frac{K_i}{s}. \quad (6)$$

Finally, applying this function to the closed loop system, the equation defining the relationship between the process output and the reference can be defined as:

$$\frac{Y(s)}{R(s)} = \frac{C(s)G(s)}{1 + C(s)G(s)} = \frac{\frac{K_g}{\tau}(K_p s + K_i)}{s^2 + \left(\frac{K_g K_p + 1}{\tau}\right)s + \frac{K_g K_i}{\tau}}. \quad (7)$$

The denominator of a second order transfer function can be defined as:

$$s^2 + 2\zeta\omega_n s + \omega_n^2 = 0. \quad (8)$$

by using the equations Equation (7) and Equation (8), the following equations are found:

$$\omega_n^2 = \frac{K_g K_i}{\tau}; \quad (9)$$

$$2\zeta\omega_n = \frac{K_g K_p + 1}{\tau}. \quad (10)$$

The poles from the closed loop transfer function need to be dominant in relation to the zero of this function for using these equations. From these equations, by defining

the desired coefficients of the system, the gains of the controller can be defined. Finally, the settling time T_s can be calculated by the following equation:

$$T_s = \frac{4}{\zeta\omega_n}. \quad (11)$$

2.4 SOFTWARES

In this section, some tools used during this project are described and the reason for choosing them is also presented.

2.4.1 Jupyter Notebook

Jupyter Notebook is a web-based interactive computational environment for creating Jupyter notebook documents as presented by (TEAM, 2019). This open-source solution born out of the IPython Project in 2014 in the direction of supporting interactive data science and scientific computing beyond multiple programming languages.

This platform allows the user to weave together computational information (code, data, statistics) with narrative, multimedia, and graphs. This can help to generate a better understanding of the work flow when reviewing it on the future. The tool is mentioned in this document when describing the stages of retrieving information from the data base, cleaning it and preparing it to be use it in other platforms.

2.4.2 MATLAB

MATLAB numerical computing environment and proprietary programming language developed by MathWorks. This software allows matrix manipulations, implementation of algorithms, plotting data and is largely used in the control field as discussed by (MATHWORKS, 2017).

Providing an accessible platform for manipulating signal data and offering many toolboxes especially for control problems, MATLAB has been used during all stages of the control implementation. In particular, these three environments:

- System Identification: Application for building mathematical models of dynamic systems from measured data.
- Sisotool: Application for designing single-input, single-output (SISO) controllers for feedback systems.
- Simulink: Application for modeling, simulating and analyzing multidomain dynamical systems.

2.4.3 LabVIEW

LabVIEW is a software development environment and language created by National Instruments. (NATIONAL INSTRUMENTS CORPORATION, 2013) defines its main difference as offering graphs programming, in other words, it uses graphical diagrams rather than lines of text. This solution makes LabVIEW more intuitive for engineers and excellent for parallel programming.

The option for LabVIEW is its efficiency and integrating any measurement hardware and its library specialized in data acquisition and instrument control. Also, the FPGA offered by National Instruments (NI) provides the possibility of sending signal, thus, the possibility of closing the loop of the system.

Each VI has 3 components: a front panel, a block diagram, and a connector pane. The front panel is where the user can interact with the program, by setting values or monitoring indicators of the current state. The block diagram is where the program can connect the terminals to determine the data flow inside the program.

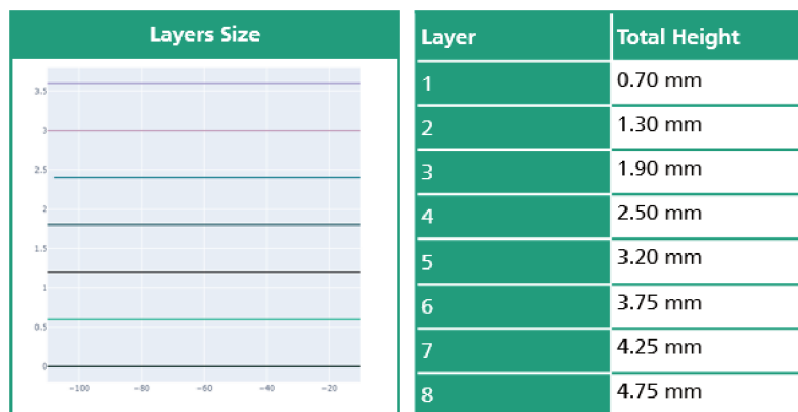
3 PROBLEM DEFINITION

As mentioned in previous sections, LMD still requires a lot of studies for creating a general knowledge of how each variable involved in this process influences the final result. From that, at this moment, there is still no mathematical descriptions of how the two selected variables for this project reacts to each other. Thus, first, open loop tests are made for developing a basic knowledge of how the system will react.

When sending a control signal, the manipulated variable is the tool end-point position. In Figure 11, it's observed how is the relation between the tool Z-Axis position and X-Axis position during one deposition. It can be observed, that for each layer, the deposition tool position in Z-Axis z_{dt} is update following the equation:

$$z_{dt_{i+1}} = z_{dt_i} + 0.6mm \quad (12)$$

Figure 11 – Position for Z-Axis in relation to X-Axis for five layers deposition



Source: Original

This value consists in the predicted height of the last layer deposited. However, it can also be seen on the table presented in the Figure 11, the measurement of the height after each deposition. By measuring the height of the bead after the deposition, it's observed that there is a difference between the height of each layer.

Thus, by adding an offset to a $0.6mm$ in each layer, a difference between the position of the deposition tool and the surface is created. Subsequently, by measuring the force during the deposition, it is possible to detect a change in the distance of the deposition tool to the bead, and, a solution for this problem can be developed.

So, for defining a method to maintain the distance between the laser and the substrate in an ideal value, the force is used for estimating this optimal position. By using the force as the controlled variable, the z position of the deposition tool is manipulated for closing the loop.

As the number of layers in a deposition grows, it can be observed an increase on the change of the measured height. This occurs because not only there is influence from the current deposition but the errors from previous layers are accumulated. As there is more change on the height, it is also expected that this reflects on the measured force.

In the Figure 12, it can be seen the first four layers of metal deposited in a bead. The process for depositing each layer is taking the wire feeder to the start position $x_{dt_{init}} = 0mm$, $y_{dt_{init}} = 0mm$, $z_{dt_{init}} = 0mm$ and moving to the negative direction of X-Axis for $100mm$ reaching $x_{dt_{end}} = -100mm$.

Figure 12 – Comparison between the dynamics through multiple layers



Source: Original

By comparing these results, the first layer presents the most different dynamics response between the values introduced. This contrast can be explained, first, by the interaction between the materials. This is the only bead that interacts directly to the substrate. In addition, as the deposition is starting, there is no influence in the temperature of previous layers in the melt pool making the response more stable.

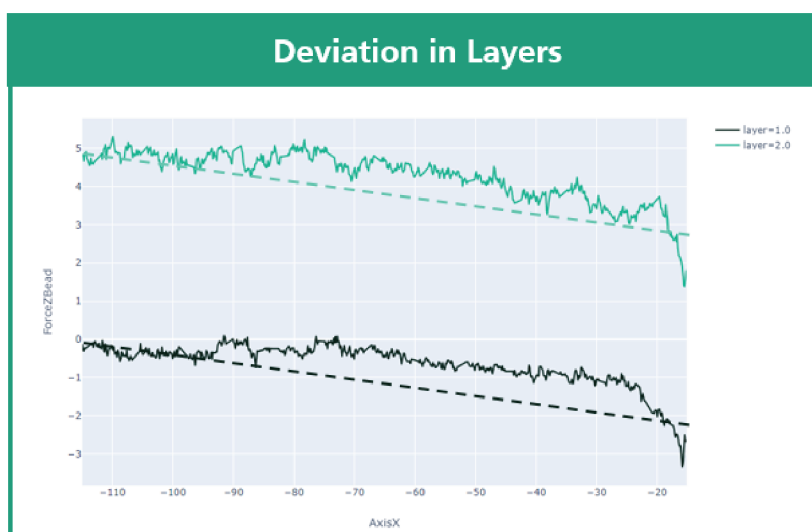
At the end, there is influence in the surface where the deposition is made. The first layer is produced in a flat surface, in contrast of the surface where the next will be produced. In consequence, the only deviation on the ideal distance between the tool and the bead will be produced if the substrate has a certain angle in relation to the tool.

In the Figure 13, the effect of this deviation can be observed. As an angle

between the substrate and the tool can only be corrected before the first layer, this error will propagate and increase between each layer. This error can happen for an incorrect axis setting in the CNC code, but it also can be caused by a natural inclination on the material.

When performing the open loop tests, this angle needs to be decreased for reaching an adequate result, however, during the close loop tests, this is a perturbation to the response that the control needs to correct.

Figure 13 – A deviation propagating through layers



Source: Original

At the Layer 2 from Figure 12, a first observation that can be made is in the increase of the force. While the first layer force is almost $0N$, the second layer has peak values of more than $5N$. Also the signal measured from this layer has more oscillations compared to the first one. From this difference on dynamics between the two layers, the necessity for multiple controls become more explicit.

In the Figure 14, the measurements of the deposition of the third layer can be observed closely. The offset from the previous layer is also $\Delta z_{dt} = 0.6mm$ summing $z_{dt} = 1.2mm$ in total offset from the base. By observing this response, it can be noted that the process has a small delay in its beginning response. Comparing to the previous layers, the force measured is bigger, certifying the tendency of forces increasing between layers, and also, the dynamics response has a look more similar to a first order system than the others.

From the Figure 12 and Figure 14, it can be observed that the second and the third layer have similar responses. The amplitude of both layers are in the range of $5N-8N$. Also, both layers have a high peak in their response before reaching its steady

Figure 14 – Forces Reaction for third layer deposition



Source: Original

value.

This peak at the beginning of the response comes from the different dynamics from the start of the deposition. However, the dynamics of this region depends on different parameters, thus, it is a difficult region to model it.

Following that, a first approach modelling the system as a second order response can be used. This model is consistently used when a system presents a damping before reaching to its final value. However, as this is a very unstable region, different tests can generate different dynamics. For that reason, a first order response, and discarding the dynamics of this region, can also lead to a good approximation.

Also, at the end of the process, a deviation from the normal response can be visualized. This effect can be seen on all the layers presented in Figure 12. The physical source of this effect can be observed in the Figure 15.

Figure 15 – Different dynamics observed on the edges of the bead



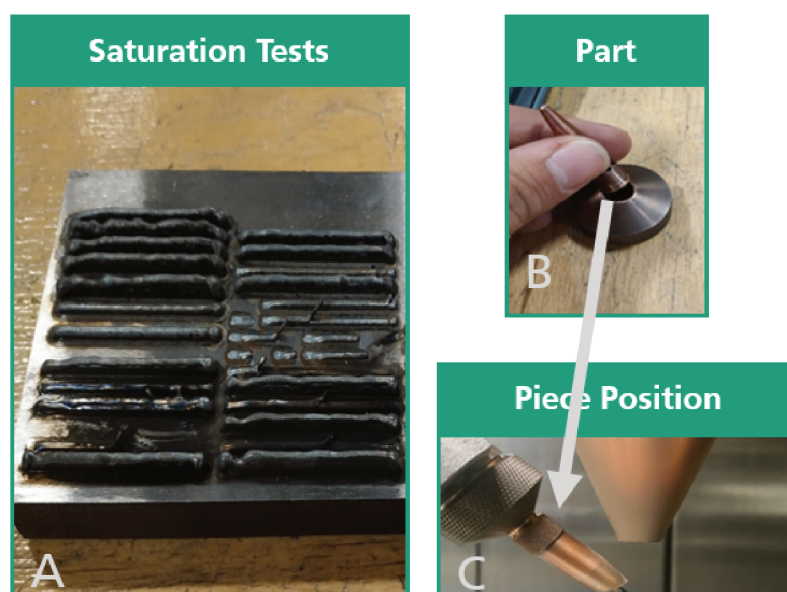
Source: Original

This presents another adversity when modelling a transfer function to this system. By not cleaning this interference during the pre-processing of the data, it can result in

an inadequate representation of the system. This region has a strategy for ending the deposition, explaining the difference in the dynamics. For that reason, the control must not be applied here.

Another limitation while applying this control is the existing physical limitations during the change in the position of the Z-Axis. As each layer height is $h_{layer} = 0.6mm$, by changing the control with a bigger value, this can result in a collision. This happened while studying the effects of this change to define a work range as seen in the Figure 16.

Figure 16 – Saturation tests during the deposition



Source: Original

Finally, a factor that influences the force during the process is the time between each layer is deposited. As each deposition increases the temperature of the part, the last layers are sensitive to this change influencing in the measured force. It was observed that a difference in the waiting time between each layer deposition changes this temperature and also effect the produced force.

All these factors need to be addressed while making open loop tests for modelling the system. For that reason, all the parameters used during this project are the same to establish a model for this set of parameters. This can be seen in the Figure 17.

Some of these variables are defined directly to the G-Code developed for the open loop tests. However, some parameters are defined in other machines, for example, the gas flow. In that manner, this needs to be verified for creating equal conditions for all the tests.

In the Figure 18, the direction of each measured force can be visualized. Two alternatives are proposed for improving the stability of the deposition. First, a combination of all the three axis is used for controlling the deposition tool position. The resultant

Figure 17 – Table describing the hardware and software parameters used during the depositions of this project

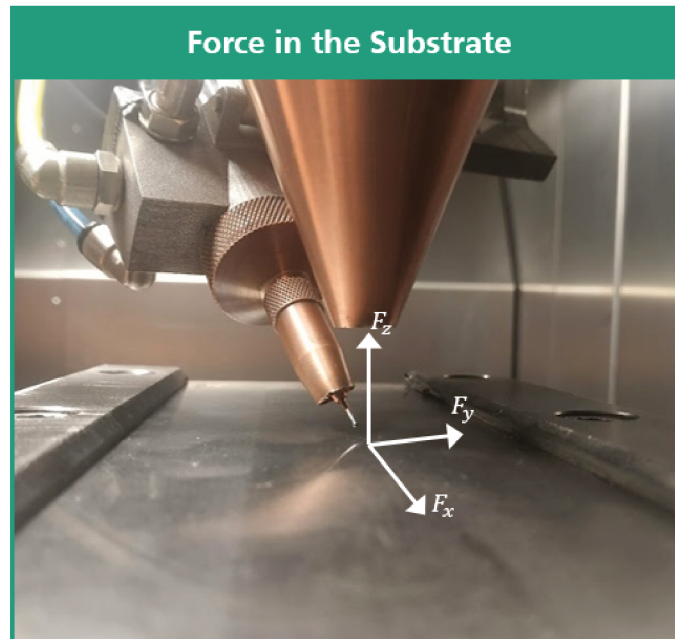
| Parameter | Value |
|-------------------------|------------|
| Laser Power | 1200 W |
| Wire Speed | 880 mm/min |
| Travel Speed | 800 mm/min |
| Gas Flow | 20 l/min |
| Waiting Time | 0s |
| Z-Axis Offset | 0.6mm |
| Direction of Deposition | X-Axis |

Source: Original

force is able to reproduce all the axis affect in the final bead. Also, a control using only the Z-Axis is proposed.

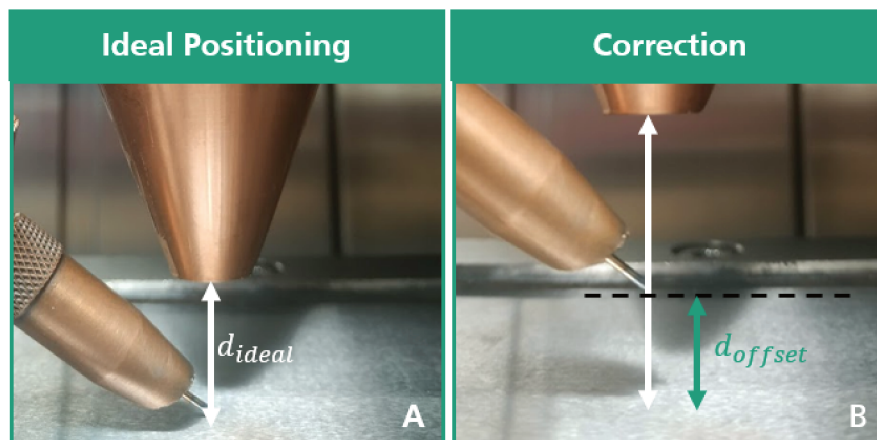
In the Figure 19, two examples of how the force affects this project. In the Figure 19-A, the tool is in the ideal position defined by the reference force. In the Figure 19-B, the deposition tool is not in the desired position. By detecting the offset between the force and the reference, this difference can be corrected.

Figure 18 – Measured Force-Axis in the deposition



Source: Original

Figure 19 – A- Ideal position of the deposition Tool; B- Deposition Tool requiring a correction



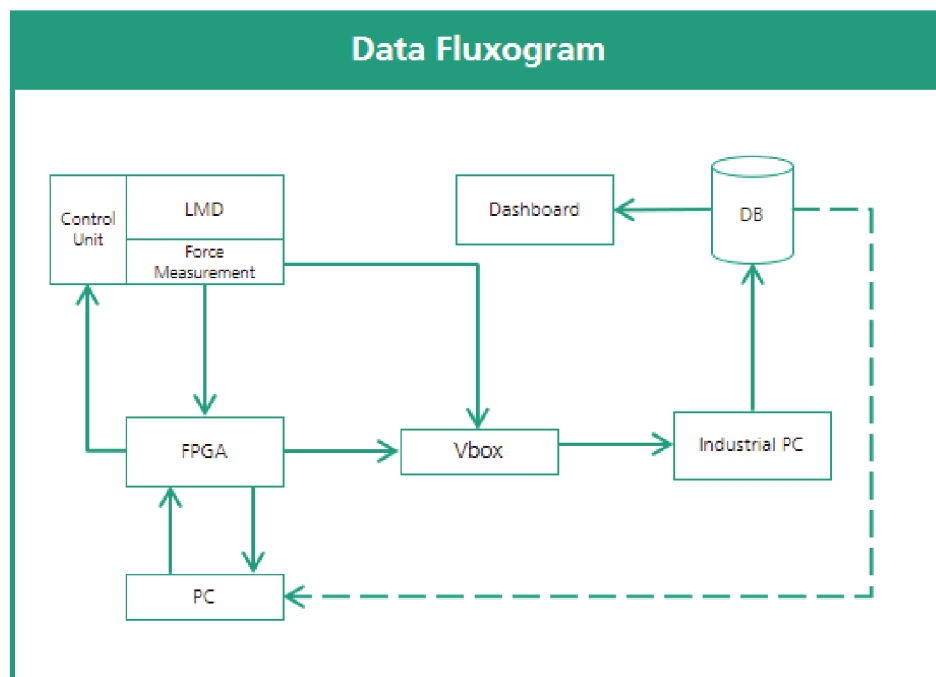
Source: Original

4 FRAMEWORK DEVELOPMENT

In this section, the developed programs for closing the loop are described. For future studies of this process, all the data collected from this process are going to be stored in a database. The hardware necessary for acquiring this information will be presented. Also, the program developed for sending this program do the database.

In the Figure 20, the steps necessary for using the data in the control are described. First, a C# software was developed for sending the data to the MongoDB. This program runs on the Industrial Personal Computer (PC) of the data flow.

Figure 20 – Path from the data observed in the Process until saving in the cloud



Source: Original

The data for this program is acquired by the acquisition system vBox. This Data Acquisition (DAQ) is connected to the FPGA of the project and the Force Measurement setup in the machine. The data from MongoDB was also used for developing an web dashboard in this project. This creates the possibility of monitoring the process from any place from the company's network.

After developing the acquisition system and the dashboard, a LabVIEW program to close the loop with the CNC machine is used. In the Figure 20, this program runs inside the FPGA. Finally a G-Code is used for receiving the signals from the FPGA. All this developed software are described on this section

4.1 DATA ACQUISITION

In this section, the necessary hardware for acquiring the data is presented. Afterward, the functionalities of the developed software is also presented. At the end, how the data is saved in the constructed database and the web dashboard is described.

4.1.1 Hardware

The applied actuators on this process are presented on the next section. The signals applied and read from the metal deposition are going to be stored in a database for further analysis. This approach is in unison with the Industry 4.0 presented on previous section.

By storing and analyzing data tests, the knowledge of its behavior increases. For this project, this data will be used for identifying the force dynamics. For acquiring all this information, two instruments are used.

First, the data is fed for two vBox. This DAQ device, seen on the left of the Figure 21 can synchronize position data and digital and analog inputs from multiple different sources. Disposing of four encoder inputs, it offers the possibility of acquiring the position from the deposition tool directly from the control unit.

Figure 21 – A vBox is seen on the left while the necessary communication card is presented on the right



Source: Original

Still, the Alzmetall is a 5-axis machine requiring one more encoder input. For that reason, one more system is used on this implementation. Developed by Fraunhofer IPT, this product can be connected to a computer using an ethernet cable. For completing this setup, a communication card is installed on the used industrial PC.

The TL100 adapter, seen on Figure 21, connect the Tria-Link to the parallel PCI bus of a PC offering the possibility of manipulating the signals by programming in different systems. Using a ring network, this communication is closed by connecting each device to exactly two other devices.

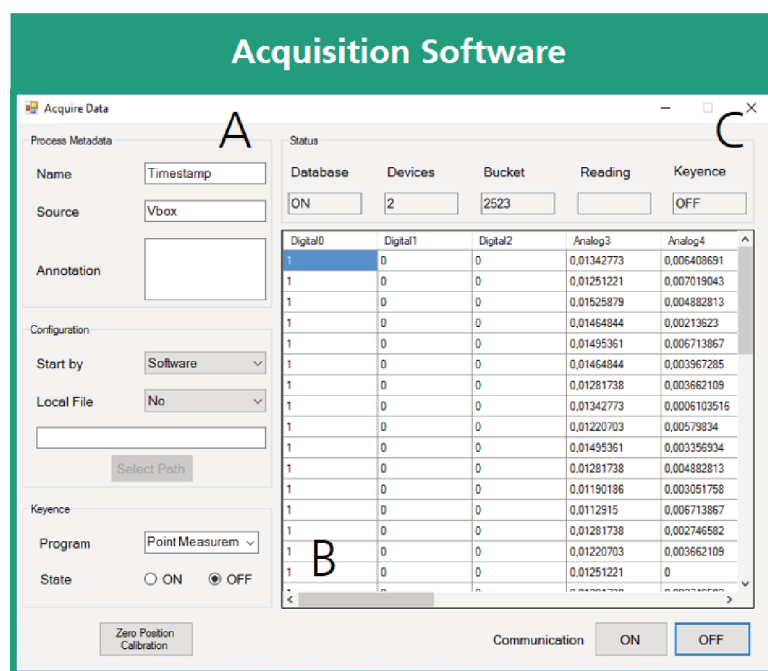
By using the analog inputs, other signals are collected as the Force and the Tool-offset control. They are all connected using the high-impedance analog input of the vBox. Also, there are digital inputs available on this DAQ, used, for example, for acquiring the state of a button to control the data flow of the following software.

4.1.2 Acquisition Software

All this hardware needs to be correctly configured for programming the signals in a computer environment. For testing the effectiveness of the connection, triamec offers a software for visualizing the data received in the card. This program also exports a configuration file for accessing the card in other programming environments.

Using this file, an acquisition program was developed in C#. This program is responsible for collecting all the data, processing it and sending it to a server. The interface developed for the operator of this program is seen on Figure 22. On this interface, the user can enter comments and other information from the tests with the purpose of identifying its properties when analyzing the results as seen on the Menu in A.

Figure 22 – Acquisition Software GUI



Source: Original

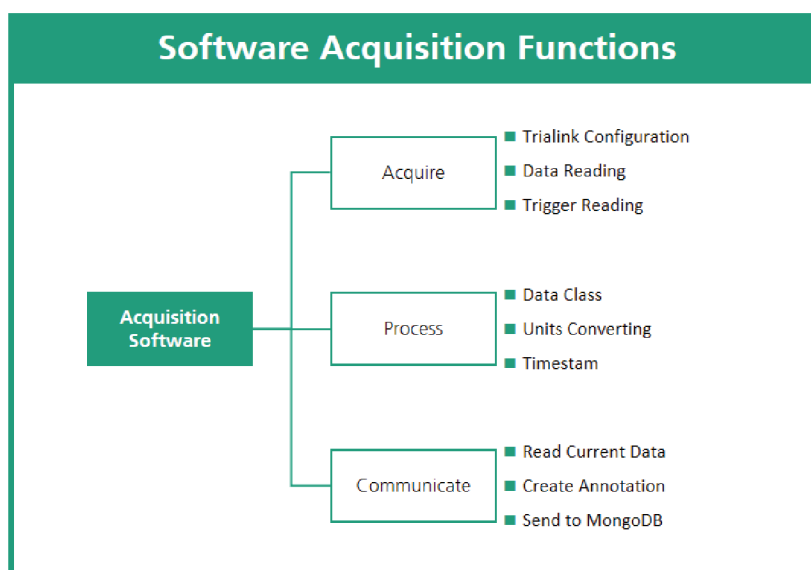
In the B section of the Figure 22, it can be seen that all the variables related to the laser metal deposition are being saved on this database, not only those used for the future control of the Force. The acquisition can be started by three ways in this software. First, the selected option on this example, a trigger sent by the software.

The operator of the software can start collecting the information by clicking the button on the bottom of the GUI. Also, a physical button sending a digital signal to the software can also be used as trigger. This two methods can be used for saving data outside the deposition window.

In the end, the acquisition can also be triggered via a signal sent by the laser source. This analog signal, sent only while the deposition is happening, can be useful for collecting only valuable data of the process. This helps on the post-processing stage of the project. From the menu located in C in the Figure 22, it can be observed the menu containing the status for the acquisition.

In the Figure 23, the three sub threads of this program can be observed. In addition to those, there is the main thread of the program responsible for initializing and closing each thread.

Figure 23 – Acquisition Software Flow



Source: Original

First, the thread containing the acquisition functions. When starting this thread, all the parameters of the communication are declared. During this step, the time between each acquisition is defined. By setting a 0.01s offset between each acquisition, a complete overview of the process is guaranteed.

The selected hardware for this project also offers the possibility of working with data packages. Thus, besides the acquisition happening in this small-time window, the communication to the program happens in a larger period resulting in a higher efficiency to the program.

After the initialization of the thread, when the acquisition is already starting, it needs to detect a change in the trigger signal. After this detection, the data is read by

the process thread.

In this part of the program, the *volts* read by the vBox are transformed into real values. In Figure 22, the table shows the data before going through this process. After the data is transformed to its units, new variables are derived from them. After this step, the data is sent to the database.

The destiny for this processed data is a MongoDB collection. This database organizes its information in base of documents. Thus, the data is transformed into a JavaScript Object Notation (JSON) structure containing the information added by the menu of the GUI. Two JSON structures are created: live data and archive data.

These structures are sent to the same database but for different collections. The live data collection only contains one document each time, for that reason, when adding the new JSON to it, the old document is deleted. This database is updated only each 500ms, period for updating the dashboard where this data is used. At the end, the archive data is sent for its own collection without deleting its old content.

4.1.3 MongoDB

The database defined for this project uses a non-relational structure. From that, the MongoDB does not need to be organized in the traditional tabular schema of rows and columns. As discussed in the previous section, there are two collections necessary for storing the data. These collections are defined in the Figure 24.

Besides using a UML class diagram to represent the database relationship, the documents inside a collection must not have all the data in the same format. For example, at the open loop studies stage of this project, setpoint was not relevant. This was only added in the final documents.

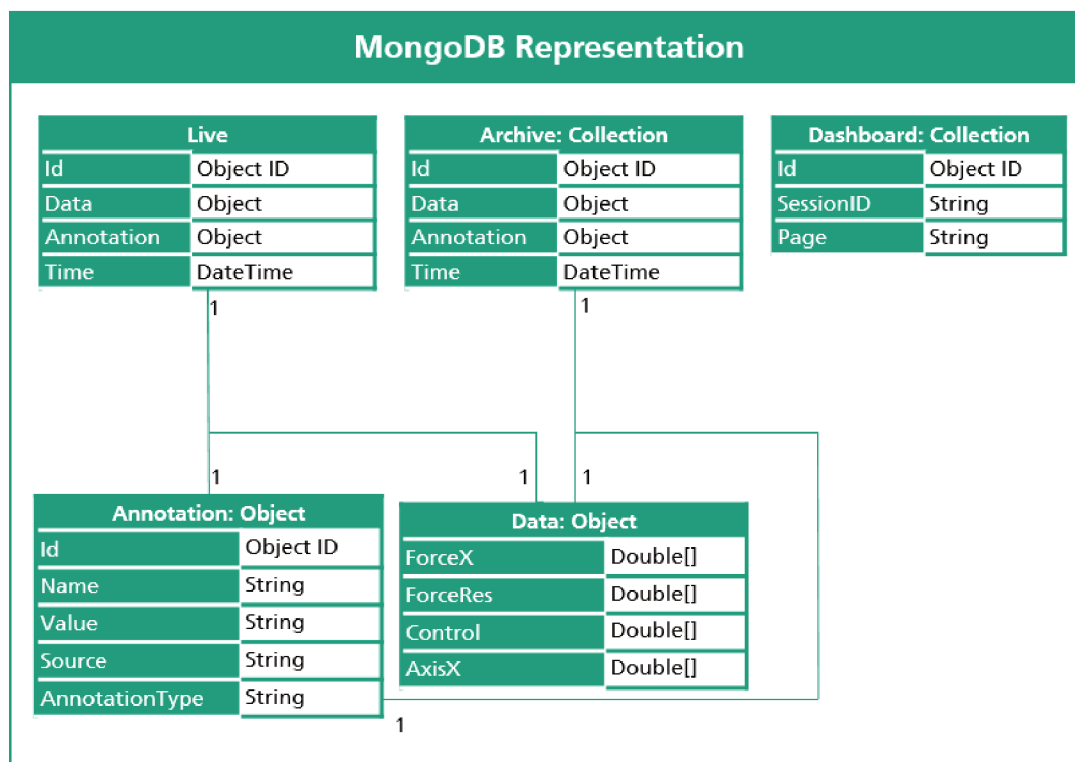
However, this change affects only inside the data object represented in the Figure 24. The structure from the collections is always the same. By maintaining this format, this database has the flexibility of including more values in the documents, and in addition, it keeps a known format helping when retrieving the data from the database.

The other collection in the Figure 24 is defined for storing the data of the usage of the dashboard. However, this collection is not defined during this project. Also, there is the representation for the data and the annotations documents. The last version of the data object has twenty variables. So, only some variables used in this project are defined in the Figure 24 for visualizing how they are stored.

4.1.4 Dashboard

Using this database, a web dashboard was developed for promptly visualization of the data acquired. From the same configuration of the MongoDB, this dashboard can use the data from the live collection or from the archive collection. In the Figure 25, the page designed for the live data can be observed.

Figure 24 – UML Representation of MongoDB



Source: Original

The bigger area of the dashboard observed in Figure 25 contains a graph displaying the current value for the Resultant Force. As this is the controlled variable, its status is the most important aspect to evaluate the performance of the control.

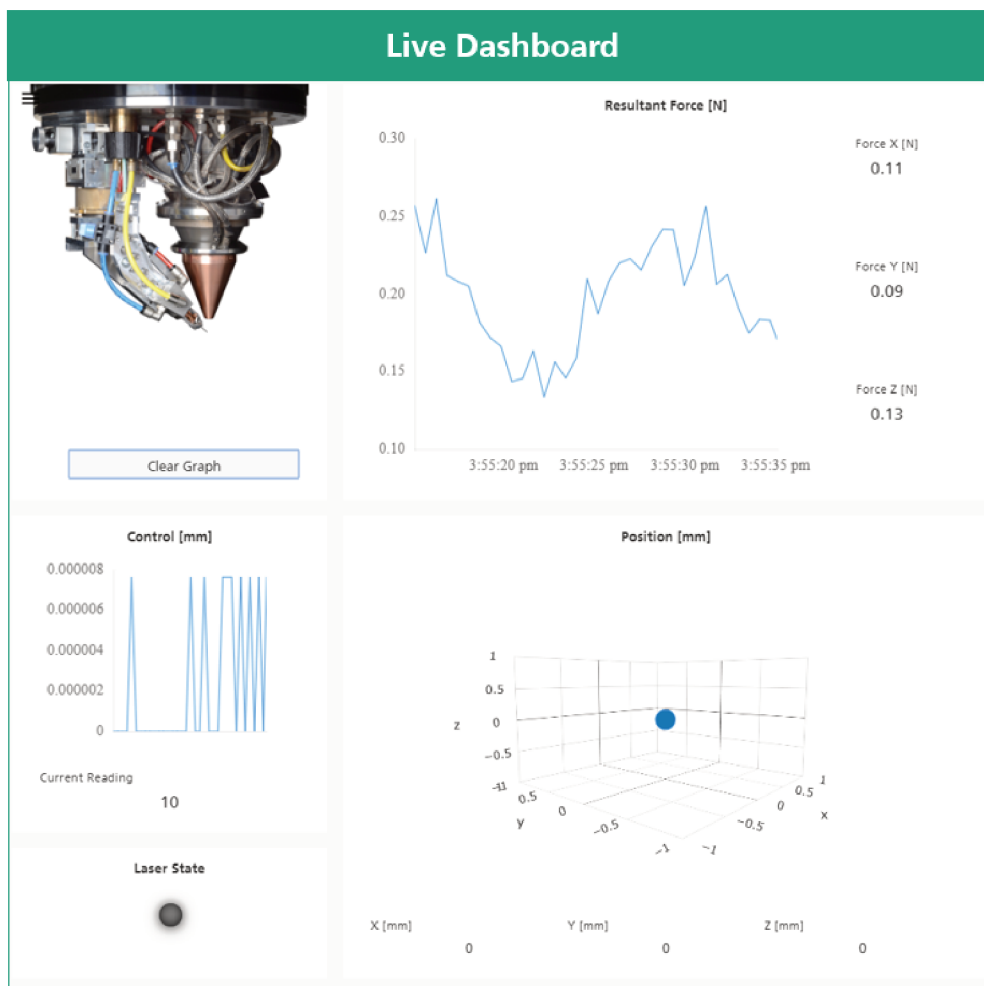
Underneath this graph, there is a 3D graph displaying the current position of the end tool. This can be used for following the deposition of the path. On the left side of the dashboard, a graph displaying the current signal that the FPGA is sending to the CNC .

At the end, a led containing the current state of the laser source underneath the control graph. The user has also the possibility of cleaning the current state of the graph using the bottom present on the left side of the dashboard or switching to the archive view in the tab menu. This other page is observed in the Figure 26.

By comparing Figure 25 and Figure 26, the layout of both pages are very similar. This layout is constructed using *HTML* and *CSS* in an *ASP.NET* framework. In addition, other libraries as *material design lite* are used for a better distribution of the panels. This library also was used when designing a mobile version for this dashboard.

As a contrast between the images, the archive mode of the dashboard has a menu for selecting the desired time frame for plotting the data. This menu is constructed using elements from the *bootstrap* library. Still, after selecting the desired time frame,

Figure 25 – Four variables that can be monitored through the live dashboard



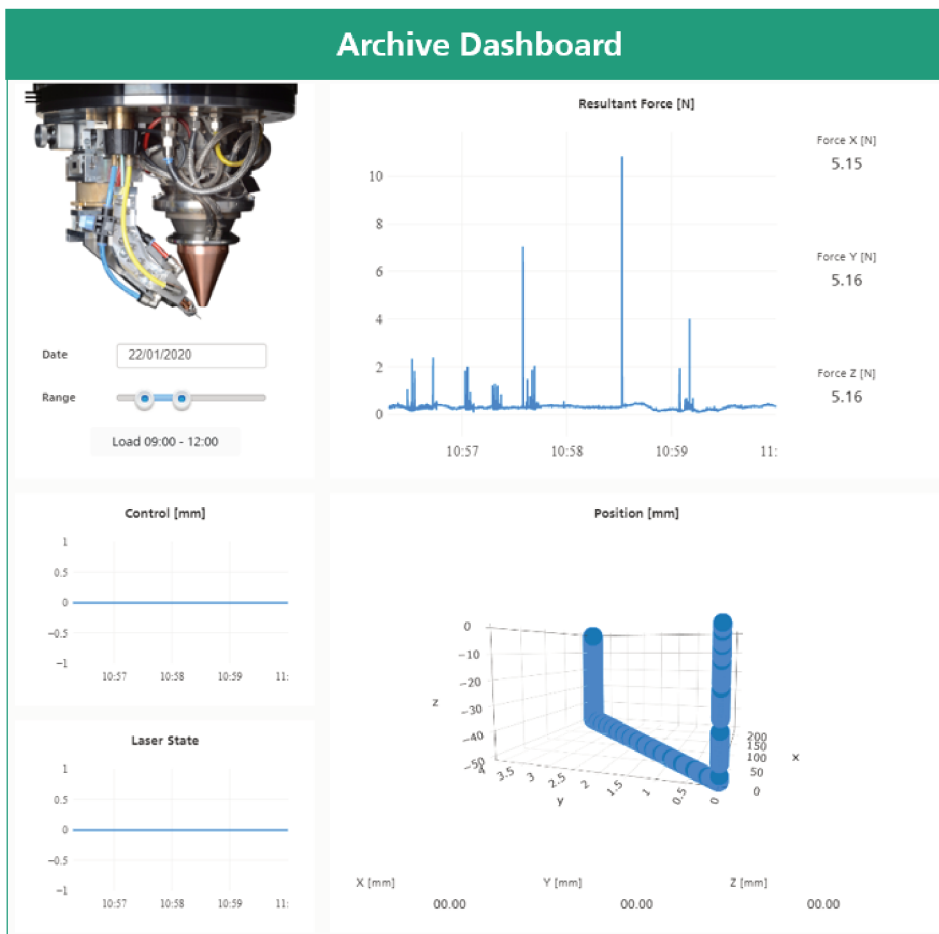
Source: Original

the data needs to be retrieved from the MongoDB.

By using the *ASP.NET* framework, each view has a controller associate to it. Inside this controller, multiple actions can be defined according to the user requests. Thus, by selecting the desired time frame, the user requests an action runned in *C#*. This action requests the data from the MongoDB and in sequence filter it for using on the graphs.

This retrieved data will be processed by *javascript* before plotting. Another difference between live and archive view is the library used for these graphs. All the graphs in the archive data uses the *plotly* library since it offers better options for interacting with the graphs. In constrast, the 2D graphs displayed on the live view uses the *chart.js* library, because it offers better performance while updating the values during the live execution.

Figure 26 – Archive Data Dashboard



Source: Original

4.2 MACHINE COMMUNICATION

During this section, the communication setup for controlling the machine will be described. The necessary equipment for acquiring the signals are presented initially. After that, the functions on the LabVIEW program used for processing them are presented. At the end of the section, how the CNC process this communication is presented.

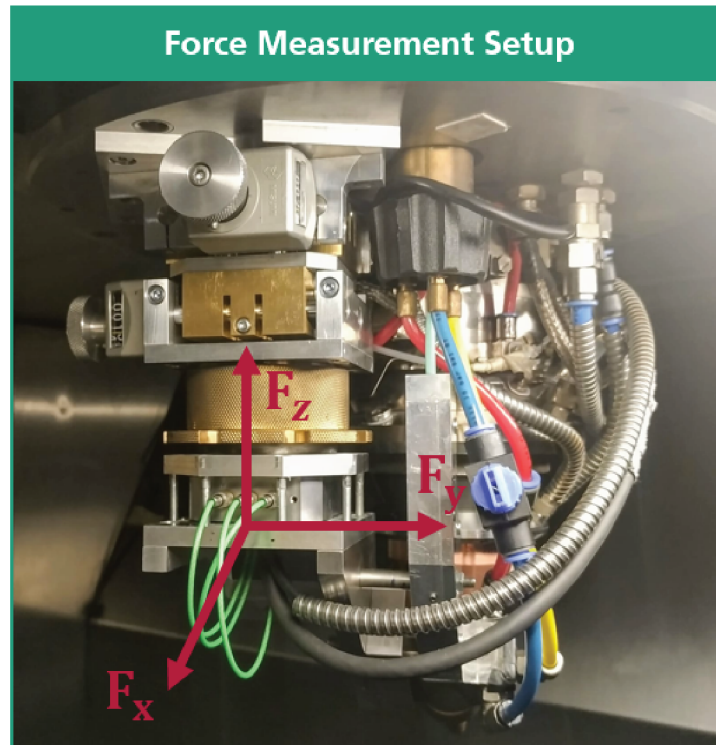
4.2.1 Instrumentation and Signal Processing

The hardware seen in Figure 27 has already been installed on the Alzmetall LOB before this project. The sensor responsible for detecting the change in the force is a Kistler 9064, which corresponds in a two steel plates containing inside of them three quartz sensors.

Each of these sensors are responsible for reading one component of the total force applied to this setup. From the Figure 27, the reference axis for the reading can

be observed. In relation to the wire arm, the Y Axis of the sensor measures the lateral forces during a deposition. The X Axis of the sensor detects the forces in the direction of the deposition. Finally, the Z Axis of the sensor detects the force in perpendicular to the deposition surface.

Figure 27 – Hardware Setup



Source: Original


In relation to the deposition direction, the sensor has a small angle. The effect of this angle needs to be verified on the study of the dynamics of this system. As seen on Figure 28, the range and sensitivity offered for the Z forces are also different. This needs to be addressed when configuring the amplifier of the system.

Besides the quartz sensors, this instrumentation also requires a 3 charge amplifier, which convert the electrical charge signals of the sensor into voltages exactly proportional to the three components. For the properly conversion, this hardware, seen on Figure 29, needs to use the values for sensitivity seen on Figure 28.

On Figure 29, the first channel from the left to the right is used for Z measurements. This can be seen by the different sensitivity from the other axis, while Z requires 3.8pC/N, the two other axis uses 8pC/N. From Figure 29, it can be seen that each 10N are transformed to 1V. As the maximal output is $\pm 10V$, the same from the FPGA used, the range for this measurement is of $\pm 100N$,

For converting this value to a computer, A FPGA from National Instruments is

Figure 28 – Datasheet Information from the Force Sensor

| Force Measurement Equipment | | | | |
|---|--------------------|------------|------|----------------|
|  | Range | F_x, F_y | kN | -20 ... 20 |
| | | F_z | kN | -40 ... 40 |
| | | F_z | kN | 0 ... 200 |
| | Overload | F_x, F_y | kN | -22/22 |
| | | F_z | kN | -44/44 |
| | | F_z | kN | 240 |
| | Threshold | | N | <0,01 |
| | Sensitivity | F_x, F_y | pC/N | ≈ -8 |
| | | F_z | pC/N | $\approx -3,8$ |

Source: (KISTLER, n.d.)

Figure 29 – Hardware used for transforming force into voltages



Source: Original

used. Seen on Figure 30, this hardware offers the possibility for combining multiple module slots depending on what type of signal is necessary to process or to send. After combining the slots, these signals can be sent for the LabVIEW program by an ethernet cable reaching a communication rate of 10 Mbps as seen in (NATIONAL INSTRUMENTS, n.d.).

Using the feature of adding slots, an analog input module is used for acquiring the signals from the amplifier. As seen on Figure 31, the input module for the NI9215 is $\pm 10V$. It also offers an acquisition frequency of 10kHz. This value will be used when applying a filter to this system.


In the end, an analog output module is also used on this configuration. The NI9269, seen on Figure 32, offers an output of $\pm 10V$ that is used for sending the tool

Figure 30 – FPGA A- Acquisition Module; B- Control Module; C- Ethernet Communication



Source: Original

Figure 31 – Datasheet Information from the Acquisition Module

| Acquisition Module | | |
|---|-------------------------|---|
|  | Number of channels | 4 analog input channels |
| | ADC resolution | 16 bits |
| | Type of ADC | Successive approximation register (SAR) |
| | Input range | ± 10.0 V |
| Conversion time | | |
| | Channel 0 only | 4.4 μ s |
| | Channels 0 and 1 | 6 μ s |
| | Channels 0, 1, and 2 | 8 μ s |
| | Channels 0, 1, 2, and 3 | 10 μ s |

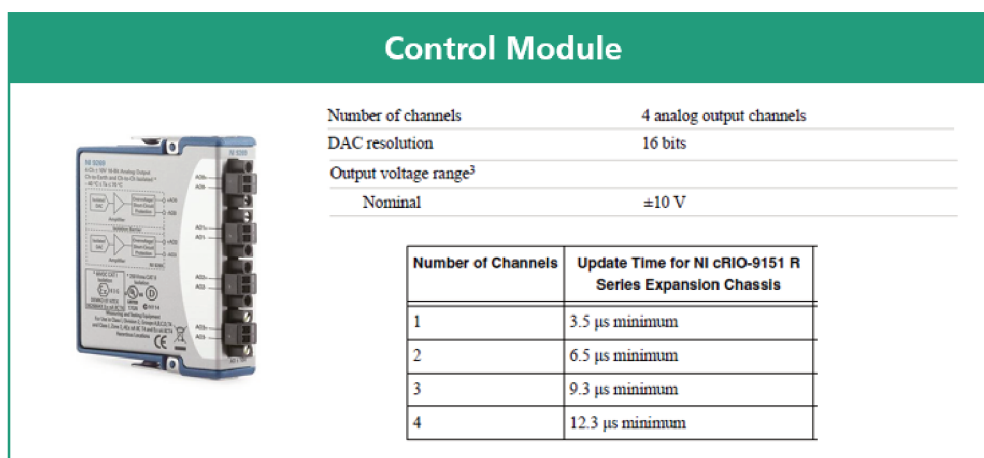
Source: (NATIONAL INSTRUMENTS, 2016a)

length correction to the G-code of the machine.

4.2.2 Labview Program

For processing the signals to display to a local operator and for calculating a control signal, the selected FPGA offers the possibility of programming in LabVIEW.

Figure 32 – Datasheet Information from the Control Module



Source: (NATIONAL INSTRUMENTS, 2016b)

This language has a special toolbox for programming in conjunction with cRio.

Using this special toolbox, the developed software is divided in two, where one Virtual Instrument (VI) runs inside on the FPGA and another runs in the local computer used for communicating with it. As described in previous section, the virtual instruments consists in two main elements, but only the program for the computer has a developed GUI.

The fast clock which cRio operates makes an advantage for acquiring the signals from the process without losing any information. However, the maximum frequency from this equipment is bigger than the frequency necessary for some of its functions to process. In that manner, this programs runs each 0.0001s.

Most of the calculation happening inside this program are inside the FPGA VI. The PC performance has decreased when some of this function were implemented on its VI, thus, its main function are displaying the results in a screen. The flow for the data in the FPGA can be seen in the Figure 33.

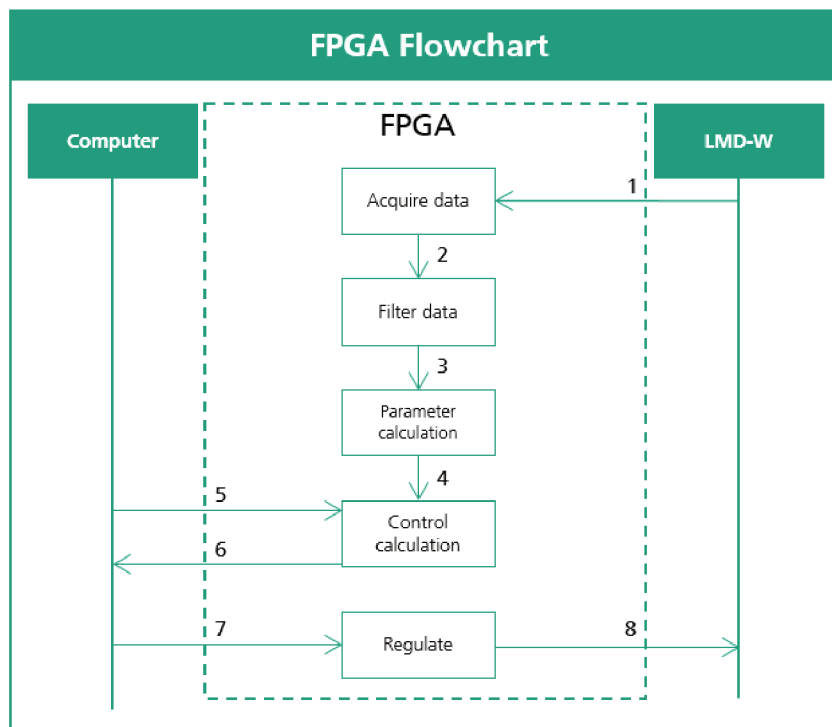
This represents the main loop of the LabVIEW VI. Before reaching this state, the FPGA needs to be initialized and its configuration setup defined. After completing this step, the FPGA starts reading the data from the Kistler amplifier. This is represented in the arrow 1 from the Figure 33.

After acquiring the data, in the arrow 2, the raw data is sent for the filtering function of the VI. Then, this filtered data is used for calculating the Force Resultant F_{res} of the measurement using the following equation:

$$F_{res} = \sqrt{F_x^2 + F_y^2 + F_z^2} \quad (13)$$

Inside the next diagram block, the arrow 5 represents the user entry for the

Figure 33 – Data flow inside the Labview VI



Source: Original

control. An example is the definition of the setpoint. Using these parameters, the FPGA uses the values coming from the arrow 4 to calculate the new control action. After that, this control action is sent for the computer on the number 6 in the Figure 33.

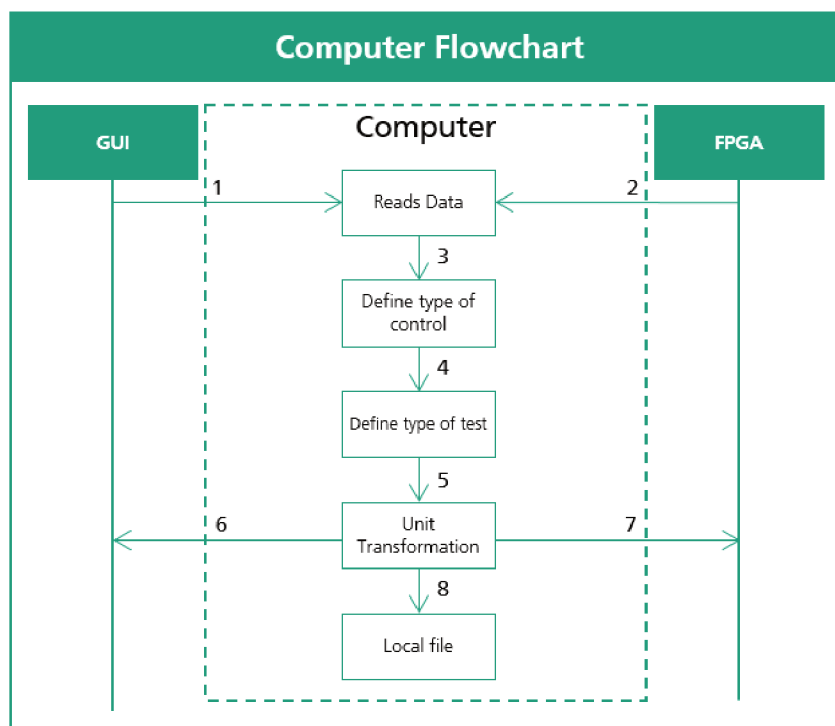
Finally, the PC selects the desired control and converts this to an electrical voltage using the range $\pm 10V$. This value is sent from the FPGA back to the process actuators. This can be seen in 7 and 8 in the Figure 33.

The data flow inside the computer VI can be seen in the Figure 34. Comparing with Figure 33, the data read in 2 in the PC flow is the data that the FPGA sends in 6. Also, the defined control that the computer returns to the FPGA is represented in 7 in both figures.

In contrast to the FPGA VI, besides their communication, the PC communicates with a user interface. In 1, the flow of the parameters defined by the user in the GUI is represented. In addition, the calculated data are displayed in graphs. This is represented in 6.

Besides reading the function to the user and the FPGA and returning the calculated values to them, the computer offers the possibility of saving the data from a test in a local file. This is represented in 8 in the Figure 34, happening after all the functions of its main loop are concluded.

Figure 34 – Data flow inside the Computer VI



Source: Original

The program sends four values to the local computer: A signal corresponding to each of the 3 forces components and the calculated control action. In the PC vi, the main functions is to return the control and display these values in a dashboard. In addition, there is also a function for local storing this information.

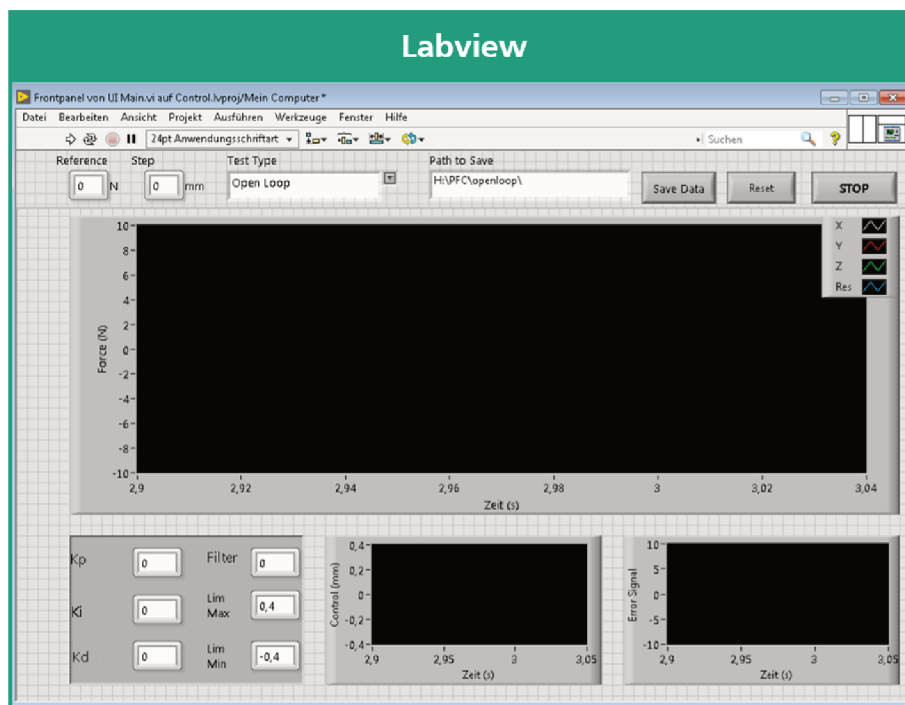
In the Figure 35, the user interface of this program can be observed. As from the web dashboard, the bigger piece of the screen is also used for displaying the force measurements. Beneath this graph, there are two small graphs displaying the control action and the error of the current state of the process.

On the same row, at the left, the parameters for the control can be defined. These parameters are used in the stage 3 of the Figure 34. The saturation of the control can be modified during the process, however, as covered by the next chapter, a default value is defined.

Nonetheless, this program can be also set for running in an open-loop test. The operating mode is defined by the user in the Test Type combo-box present in the menu in the upper portion of the screen. There are three main options: Open loop, resultant force control and z force control.

Finally, the setpoint of the control can be defined by the user or the amplitude of the change in the actuator signal in a step test. This can be seen in the upper menu in the Figure 35. These inputs are used when defining the new control in the stages 3, 4

Figure 35 – LabVIEW GUI



Source: Original

and 5 of the Figure 34. The final actuator value is sent for the CNC used for controlling the deposition.

4.2.3 CNC

A conventional 5-Axis machine tool from Alzmetall is adapted to this LMD process. In the Figure 36-A, the panel from the machine can be seen. This is where the user can program the G-code and use the other controls to interact with the process. In the Figure 36-B, the processing head of this setup can be visualized.

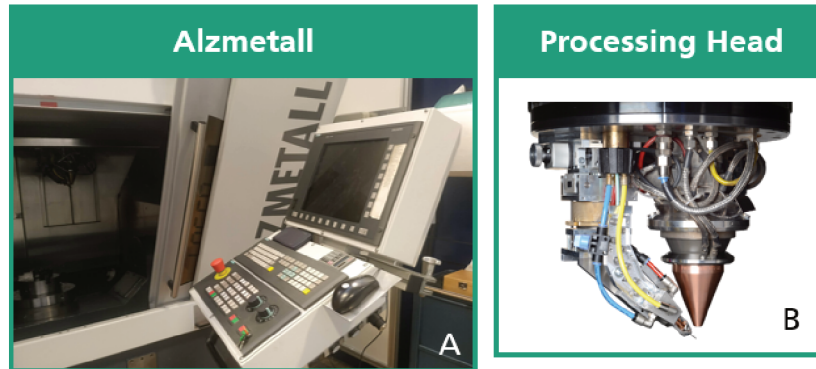
4.2.4 G Code

All the tests are done using this code while receiving the input signal from the LabVIEW programmed in the previous section. This signal is read by the CNC as a 16-bit integer and needs to be processed during the G-Code.

The most significant bit from this value represents the reading signal. So, after reading this value, three conditions for the correction of the tool offset is defined: positive steps, negative steps and zero. This is possible through the synchronized actions available in the sinumerik 840D as seen in (SIEMENS, 2012).

In synchronized actions, tool length compensations can be applied in all three

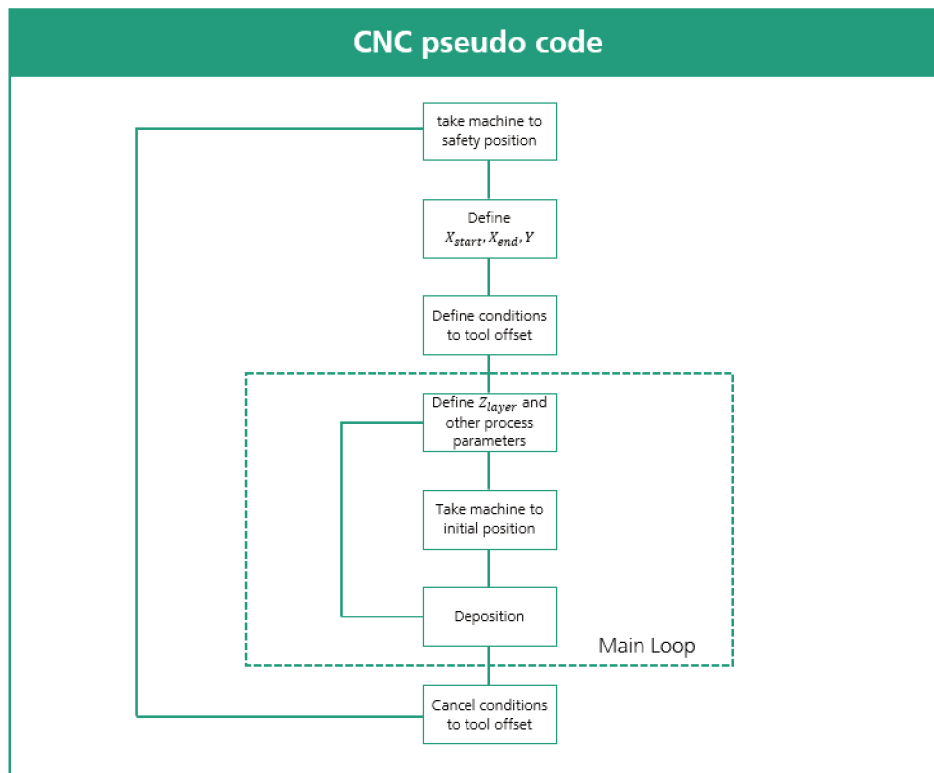
Figure 36 – The CNC Panel and the processing head of the LMD setup



Source: Original

dimensions. The code must switch this compensation on by writing the line *TOFFOF(Z)*. This means that only the Z-Axis will be modified. In the Figure 37, this line is displayed on the "Define conditions to tool offset" block. Also, when finishing the deposition, this compensation must be turned off as seen on the last block of the pseudo code.

Figure 37 – Pseudocode from the G-Code used during the open loop depositions



Source: Original

The only difference between the open loop g code and the closed loop is during the definition of the conditions to the tool positioning correction. For the closed loop tests, the tool correction is defined by the value sent by the FPGA during all the deposition. In contrast, on the open loop, the correction happens only at the middle of the bead, assuring where the step signal will be generated. This is defined using the current position variable AA_IW of the tool.

First, the initial conditions of the axis are defined. From this, the final size of the bead can be determined. For having enough time for identifying where the force reading accommodates, the length of the bead used is $100mm$. After defining this values and also defining the conditions for the tool correction, the machine is taken to its initial place.

During the deposition, the G-code also controls the start of the laser, the gas flow and the wire feeding. Thus, when the deposition starts, first the g code defines the start of the gas flow, then after a small pause, the laser source is turned on and lastly the feeding of the wire starts.

When finishing the deposition, the inverse action is necessary. So, first, the code stops the wire feeding, in the sequence, it turns the laser off, and at the end, it closes the gas valves. This sequence is the same for all the layers happening in the Deposition block in the Figure 37.

After this block, the main loop continues until the maximum number of desired layers is reached. When the current layer is smaller than this threshold, the offset of $\Delta z_{dt} = 0.6mm$ is added to the Z-Axis and a new process starts.

5 FORCE CONTROL

In this chapter, the steps necessary for closing the loop are presented. At the first section, the identifying of the system is discussed. By using these models, on the next section, the parameters of a PI control are calculated. At the end, the results are discussed.

5.1 SYSTEM IDENTIFICATION

Two methods for identifying the system are proposed. As the only correction applied to the tool is on the Z direction, a control using the Z-Force as a process variable will be defined. Also, a control using the three-axis impact in the force is inspected to see which one offers a better result.

5.1.1 Resultant Force

When starting an open loop test for the laser metal deposition, it is necessary to define in which layer this will be done. As discussed, each layer presents a different dynamics, suggesting the necessity for creating different transfer functions.

Nevertheless, a generalization for this dynamics will be presented as a first study on the possibility of controlling this system. As discussed, the first layer presents the most different dynamics from the deposition. For that reason, this is not the ideal selection when creating a generalization for this system.

For being the first layer where the interaction of the deposition occurs in the same material surface as the following layers, the second layer is for creating a generalization. On the second layer, it is expected that the force does not suffer as much effect from the deviations on the surface as the following layers.

Also, by studying the open loop responses, the third layer dynamic has similar shapes than the following layers, despite the fact that the following layers have higher forces. The effect of a step happening on the third layer is also considered.

By decreasing the deposition tool position value $\Delta Z_{dt} < 0$ and registering these readings in a database, the method used for verifying the dynamics of the system is a black box method. As there is no phenomenological (physycal) basis to create the model, the system will be defined using the two following models:

$$F_{res} = \frac{K_p}{\tau s + 1} * \Delta Z_{dt} \quad (14)$$

and also:

$$F_{res} = \frac{K_p}{(\tau_1 s + 1)(\tau_2 s + 1)} * \Delta Z_{dt}. \quad (15)$$

The first order representation, defined in equation 14, is made by plotting the graph and calculating the variables using the equations defined by Hägglund:

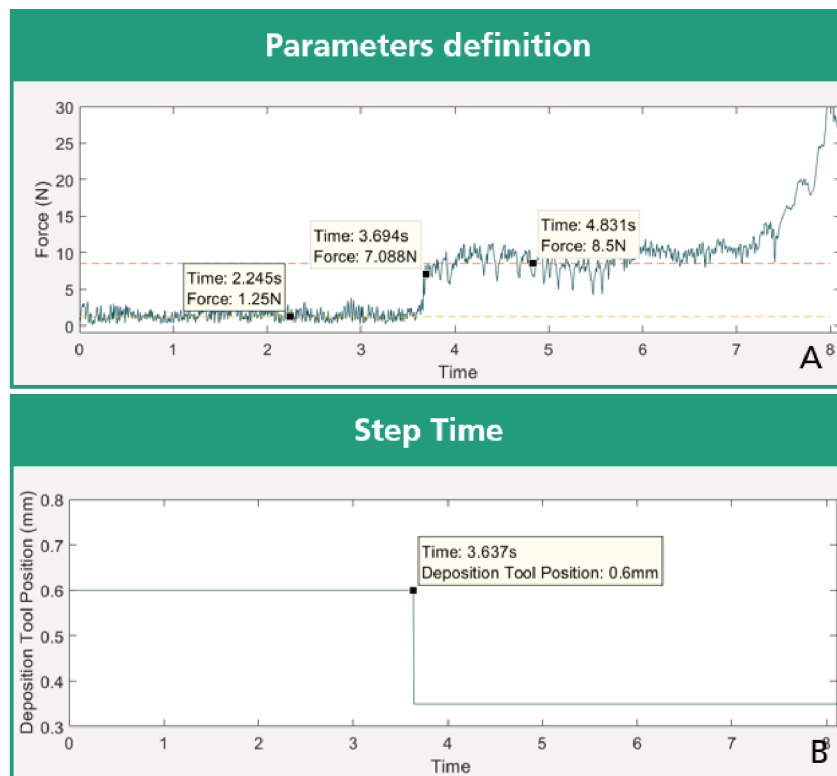
$$K_p = \frac{\Delta y}{\Delta U}; \quad (16)$$

$$\tau = t_2 - t_1. \quad (17)$$

where t_2 is when the value of y is equal to $0.63y_f$ and t_1 is the instant that the change on the signal happens.

In the Figure 38, a first order identification using the second layer step is presented. The total time t_{total} of this step is 8,4 seconds. So, at the middle of the deposition, at the time t_{step} of 3,6 seconds, after the resultant force reached a stable value, a step Δz_{dt} of -0,25mm is added to the system.

Figure 38 – Using matlab plot for defining the system parameters



Source: Original

Also, the resultant force measured is displayed in the Figure 38. Before the perturbation is added to the system, its output F_{t1} is approximately 1.25N. After changing the control signal, the measured force F_{t2} is around 8.5N. So, by applying the Equa-

tion (16), the gain of the transfer function can be defined, as following:

$$K_p = \frac{\Delta F_{res}}{\Delta z_{dt}} = \frac{7.25}{-0.25} = -29. \quad (18)$$

Also, the system response reaches 63.2% of its final value at the instant $t_{0.63y} = 3.693$ seconds. Therefore, the time constant τ can be calculated by applying the Equation (17), as following:

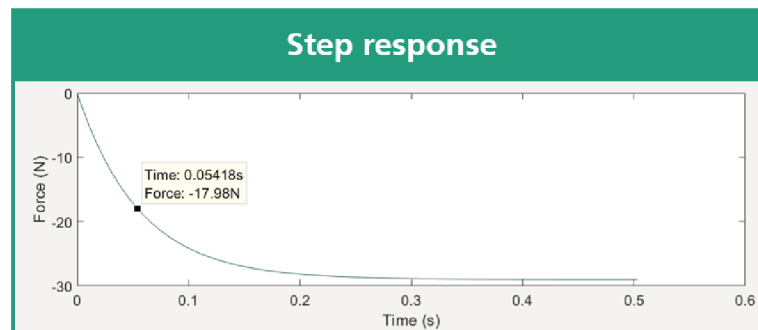
$$\tau = t_{0.63y} - t_{step} = 3.693 - 3.639 = 0.054. \quad (19)$$

Using the equation Equation (14), the resultant force system is defined by the following first order transfer function:

$$G_{res_{11}}(s) = \frac{-517.85}{s + 17.85}. \quad (20)$$

From the Equation (20), the model has an inverse response transfer function, in order words, when the control signal decreases, the process variable increases. Also, by the position of the pole $p = -17.85$, the expected time response for a step is very short. The unitary step for this model can be seen in the Figure 39.

Figure 39 – Unitary step response for equation Equation (20)



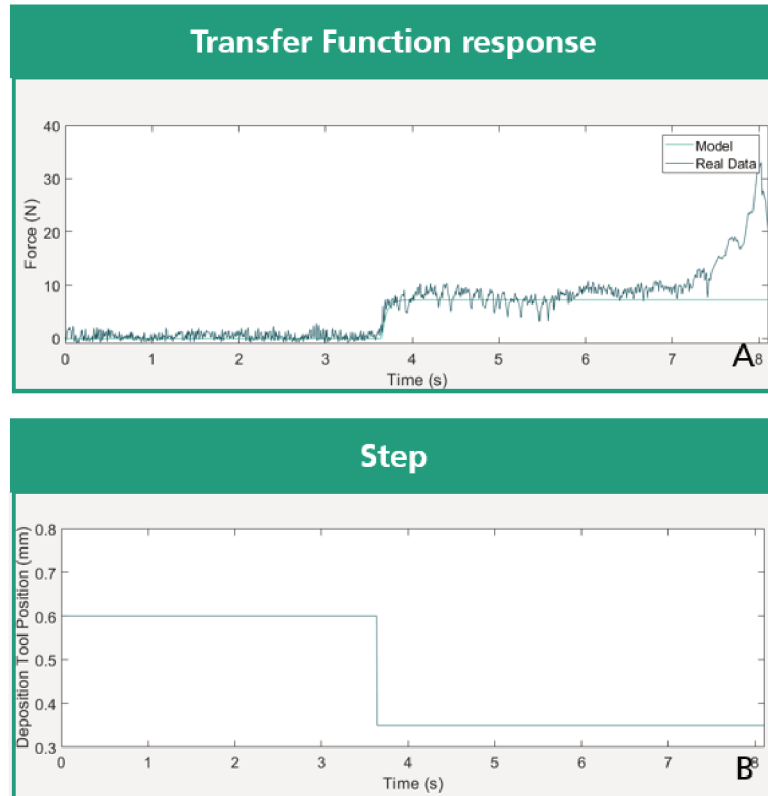
Source: Original

In the Figure 40, a graph displaying the acquired data from the step used for identifying the system and also the simulated data using the transfer function Equation (20) can be seen. From this image, the selected pole has a good representation for this system, as the simulation data time response is very similar to the acquired data.

Also, besides at the end of the deposition, the amplitude of the force response is well represented. As discussed in previous sections, the end of bead has a different dynamics, so, this dynamics must not be considered when the result is considered.

For comparing the transfer function of the second layer, a study using the third layer will also be used. In the Figure 41, the data acquired during this test can be

Figure 40 – Simulated and real step response



Source: Original

visualized. In the graph A, the position of the deposition tool can be seen. In the first layer, the end point position is $x_{dt} = 0mm$.

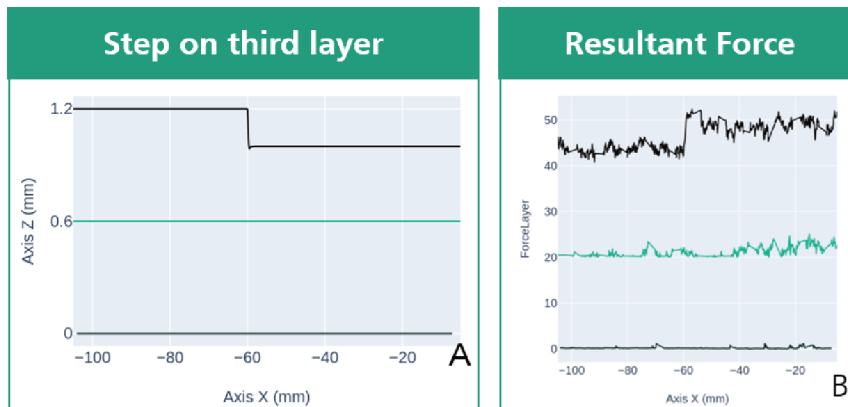
As the number of layers are growing, an offset of 0.6mm is added between each deposition. At the third layer, a step of $\Delta z_{dt} = -0.2mm$ is added to the input. The effect of this perturbation can be seen on the graph B of the Figure 41. This graph displays the resultant force in each layer with an offset of +20N in each deposition.

In the Figure 42, the data used for identifying a first order system in the third layer can be visualized. Before the perturbation, the mean force is $F_{res} = 2.5N$, while after the change in position of $\Delta z_{dt} = +0.2mm$, the force increases reaching approximately $F_{res} = 8N$. Comparing the values from the Figure 42 to the Figure 38, a notable higher oscillation can be detected. This can be explained by an uneven surface from the previous layers.

By using the same equations to define the transfer function, and by knowing that the step happened on the instant $t_{step} = 2.538s$, while the response reached 63.8% of its final value at the instant $t_{0.63y} = 2.588s$, the transfer function to this data is:

$$G_{res_{12}}(s) = \frac{-550}{s+20}. \quad (21)$$

Figure 41 – Graphs Displaying the position and the force in three layers



Source: Original

This equation has similar values to gain and pole in comparison to the transfer function defined in Equation (20). Although, they have expected similar output, the equation defined from the second layer is much more trustworthy as the oscillation is lower than on the present in the third layer.

Finally, a second order model will be defined for comparing all the outputs. This transfer function is modelled using the toolbox system identification of Matlab. This toolbox allows the user for creating multiple tests datasets before running the algorithm for approximating to a transfer function. By applying this function, it is possible to model the system through data from different layers.

When using this function, it is necessary to consider the sampling time used for acquiring this data. All the data used for creating a mixed dataset used a sampling time of $t_{st} = 0.01$ s. The first equation defined by this toolbox was:

$$G_{res_{21}}(s) = \frac{-69240}{s^2 + 37.73s + 2838} \quad (22)$$

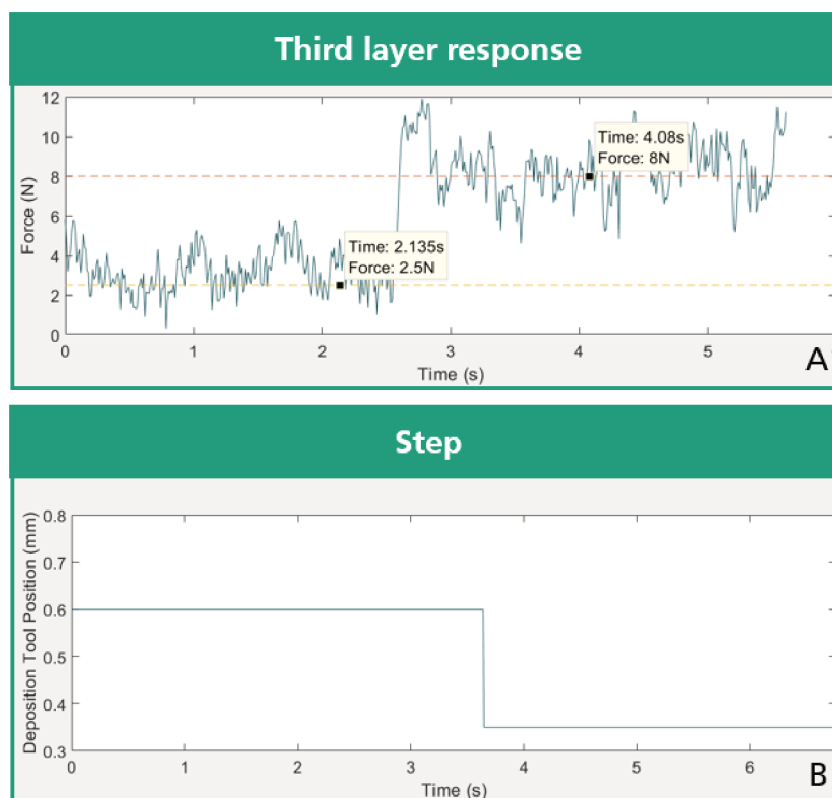
As seen in the Figure 43, this transfer function has a high overshoot to a unitary step. This is explained by its conjugated complex poles $p_{1,2} = -30.60 \pm 57.75j$.

In this Figure, it is also observed that all the models have similar outputs. While the transfer functions generated using *Matlab* has a slightly low gain compared to the other equations, all the steps have similar settling time. As in Figure 40, the step using a model is already compared to the real data, it can be concluded that all the transfer functions represents the system well.

5.1.2 Z Force

As an alternative, a control directly to the Z-Axis will also be applied to this process. The same technique for modelling applied to the resultant force will be used

Figure 42 – Acquired data used for identifying a first order function



Source: Original

for this identification. First, a step is introduced to the system as seen in the Figure 44.

Comparing to the observed response of the resultant force, the variation in the amplitude of the force is a notorious contrast in this test. While the steps produced in the resultant tests have amplitudes above 5 Newtons, in this case, it is observed an amplitude of approximately 1N.

After the calculations, the obtained first order models to this variable are:

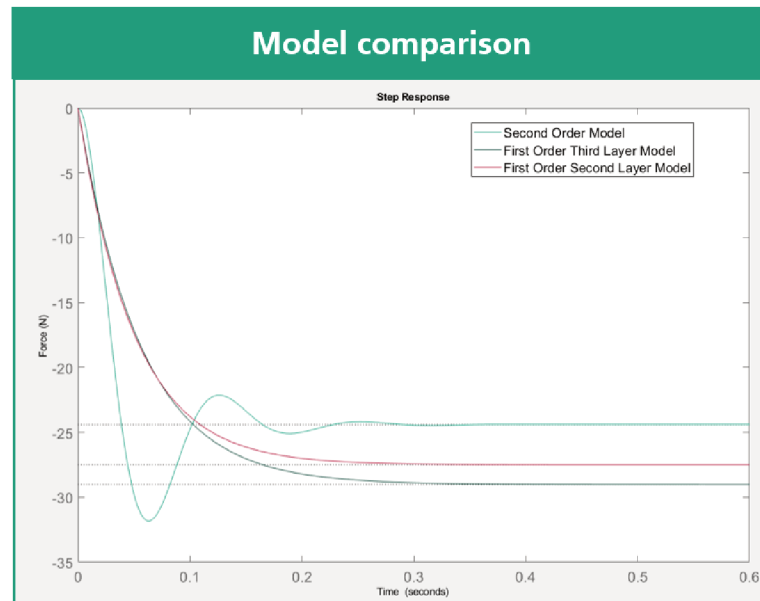
$$G_{z_{11}}(s) = \frac{283.475}{s+66.7}; \quad (23)$$

$$G_{z_{12}}(s) = \frac{111.1}{s+22.22}. \quad (24)$$

In the Figure 45, a comparison between the real data observed when a step was added to the system and the model output to the same step. The amplitude from the model is very similar to the final value from the real data. Also, the rise time is fitting to the system. However, the real system has a lot of small oscillations that the first order model is not able to demonstrate.

A second order transfer function is able to model this damping in its response. As in the resultant force, using the system identification toolbox, the following equation

Figure 43 – Multiple Plots from different transfer functions to this system



Source: Original

is obtained:

$$G_{Z_2}(s) = \frac{16210}{s^2 + 34.86s + 3663} \quad (25)$$

In the Figure 46, the step response of these three models are demonstrated. By comparing these values, it can be observed that all have similar amplitudes in their response. These values are in the range of 4N and 5.25N.

Also, it can be concluded that this model has similar settling time after a step. These values are in the range of 0.05s and 0.15s. As in Figure 45, a contrast between a model and the real data is already analyzed, it can be concluded that all the transfer functions have similar responses to the system.

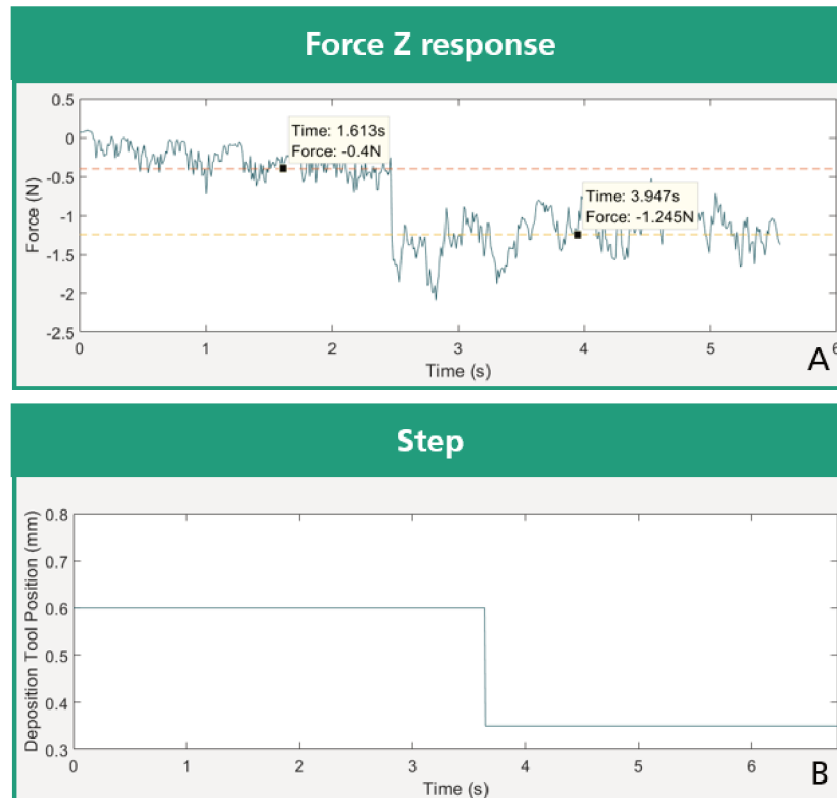
5.2 CONTROL DESIGN

In this section, the selected control designs for this system is presented. First, the limitations and the assumptions made are introduced. After that, the equations for each model are presented and its results are compared. At the end, alternatives are proposed.

5.2.1 Assumptions

One limitation from the physical tools available to this project is the control working range. As each layer has approximately $h_{layer} \approx 0.6mm$, the maximum correction

Figure 44 – Step result in the second layer for a perturbation in the Z axis



Source: Original

in each direction is defined as $\Delta z_{dt} = \pm 0.4 \text{ mm}$. This results in many limitations while applying the regulation, notably, two variables in the control are directly affected by this value.

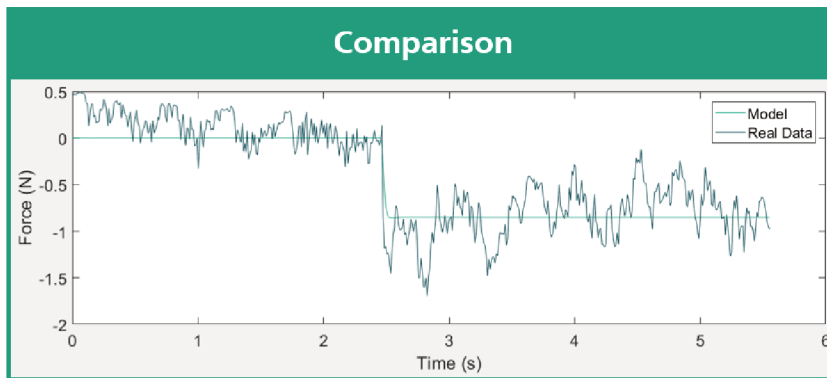
As the amplitude of the observed during the deposition reached values of more than 10N, a high proportional gain can lead to constant saturation in the process. It was observed that controllers using gains $K_p > 0.1$ have an on-off behavior in this process due the saturation. For keeping a margin of safety in this constraint, the desired value of this parameter needs to have a smaller value. Thus, this parameter is defined by the following condition:

$$K_{pdes} < 0.02. \quad (26)$$

Besides using a smaller condition, $K_p < 0.1$ also produces an adequate result. However, when calculating the control parameters, the desirable value is used.

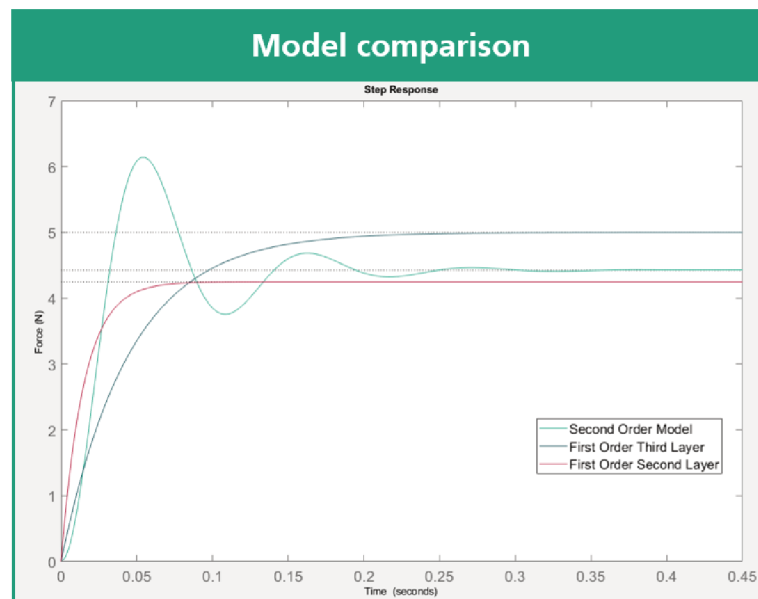
Forces inside the region of 10N are still on the working region. In an example where the error is equal to this value, the proportional correction is 0.2 mm . This represents 50% of the maximum control range. Besides the saturation, a high proportional gain causes a quick change in the control action. This changes can lead to problems in

Figure 45 – Comparison between the step using the real data and the model



Source: Original

Figure 46 – Multiple Plots from different transfer functions to this system



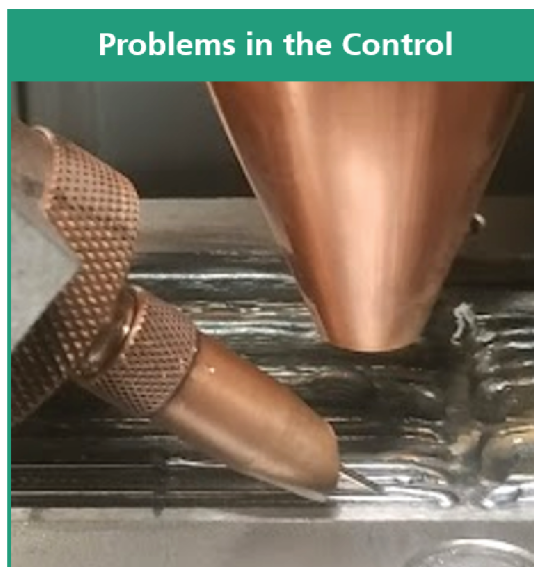
the deposition as in the Figure 47.

Also, the desire response must not have oscillations, which also can result in a saturation during the control calculation. For that reason, an underdamped system is not adequate, and in that case, the damping ratio is defined as following:

$$\zeta \geq 1. \quad (27)$$

Two alternatives are used for dealing with the windup effect observed in PI controllers. In the LabVIEW, an algorithm for automatically correcting this error can be selected. This algorithm guarantees that when the error decreases, the controller output decreases, moving out of the windup area.

Figure 47 – Problems caused by an abrupt change in the control signal



Source: Original

Also, the PI VI used in this project has a feature for cleaning the accumulated error during the execution. This can be used for cleaning the error between the deposition. The button used for this alternative is seen in the Figure 35. These both alternatives are efficient in correcting the windup effect.

5.2.2 Resultant Force

By regulating the resultant force, all the axis have influence in the final tool positioning. This leads to higher inputs to the controller, as observed in the Section subsection 5.1.1. This needs to be addressed while defining the parameters. A solution for the first order model and a solution for the second order transfer function are defined.

5.2.2.1 First Order

For calculating the first order response, the pole allocation method will be used. In this method, by comparing the closed loop equation of this system to a closed loop equation of a second order response, the parameters of the response can be defined.

As both first order models have a similar step response, the allocation of its closed loop poles does not produce a noticeably different control. For that reason, only one model is used for calculating the gains of the controller.

$$\frac{-517.85(K_p s + K_i)}{s^2 + (-517.85K_p + 17.85)s + -517.85K_i}; \quad (28)$$

$$2\zeta\omega_n = -517.85K_p + 17.85. \quad (29)$$

Using the equation Equation (26) and Equation (27), the natural frequency ω_n can be defined. The selected value for the proportional gain is $K_p = -0.01$. So, the natural frequency is defined as following:

$$\omega_n > \frac{-517.85 * -0.01 + 17.85}{2} = \frac{23}{2} \approx 11.5; \quad (30)$$

$$\omega_n^2 = -517.85K_i \rightarrow K_i \approx -0.25. \quad (31)$$

Finally, the control equation is defined as:

$$C_{res_1}(s) = \frac{-0.01(s+25)}{s}. \quad (32)$$

By finding the roots from the denominator, the poles of the closed loop transfer function are $p_1 = 13.25$ and $p_2 = 9.8$. The zero is not irrelevant in relation to these poles, influencing the closed loop response. For that reason, the dynamics of this system was investigated using the Sisotool toolbox.

5.2.2.2 Second Order

For the second order transfer function, the control was defined using the toolbox Sisotool of Matlab. As the first control using this variable, the proportional gain K_p of this equation also requires to have a low value. In the Figure 48, the tuning made in the toolbox Sisotool can be observed.

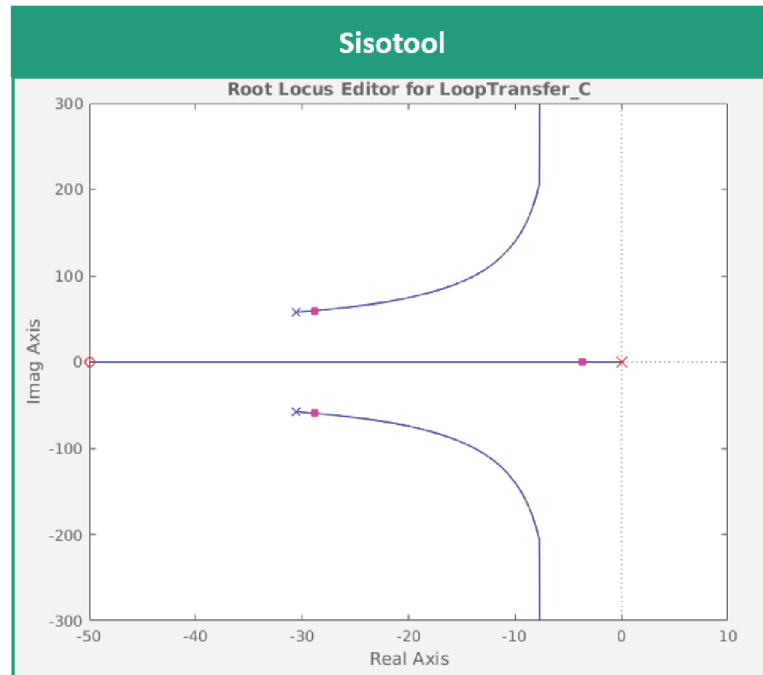
By positioning the pole with a lower real value compared to the open loop poles and defining a small K in the root locus, the closed loop have a response without oscillation. The equation defined for this controller is:

$$C_{res_2}(s) = \frac{-0.03(s+503)}{s}. \quad (33)$$

This controller also guarantees a settling time inside the deposition total time. For reaching a smaller settling time, the K_p does not follow the condition defined in Equation (26). However, it is still under the condition $K_p < 0.1$, where the control does not have an on-off behaviour.

However, this controller C_{res_2} has a slower reaction in following reference compared to C_{res_1} . This can lead to deposition problems when applying the control into the system.

Figure 48 – Using the Sisotool toolbox for tuning the control parameters



Source: Original

5.2.3 Z Force

For comparing which variable produces the better result, the models for the Z-Force are also used for tuning a control. The controls C_{Z_1} and C_{Z_2} are defined following the same methods as the controls C_{res_1} and C_{res_2} .

5.2.3.1 First Order

The closed loop transfer function of the model G_{Z_1} is defined by the following equation:

$$\frac{283.475(K_p s + K_i)}{s^2 + (283.475K_p + 66.7)s + 283.475K_i} \quad (34)$$

Comparing to the equations defined in Equation (8), the K_p and K_i of the PI have the following relationships:

$$\omega_n^2 = 283.475K_i; \quad (35)$$

$$2\zeta\omega_n = 283.475K_p + 66.7. \quad (36)$$

At the end, using the same assumptions defined at the beginning of this chapter, the final control is defined by the following equation:

$$C_{Z_1}(s) = \frac{0.01(s+425)}{s}. \quad (37)$$

5.2.3.2 Second Order

Using the equation Equation (25) and also using the Sisotool for allocating the poles of settling closed loop system, the following control was defined for the second order system:

$$C_{Z_2}(s) = \frac{0.004(s+100)}{s}. \quad (38)$$

5.2.4 Results

Using the presented controllers, beads were deposited for analyzing which variable and which model produces the best response. In the Figure 49, a comparison between the force response applying each control in the second layer of a deposition is demonstrated.

Figure 49 – Force in the second layer



Source: Original

For the beads produced using resultant force as the process variable, seen in the Figure 49-A and -B, the setpoint is defined as 5N. In contrast, the beads produced using the F_z , seen in the Figure 49-C and -D, the selected setpoint is -1N. This can be verified looking at the green line in each graph. These values are empirically selected by observing the force in open loop tests.

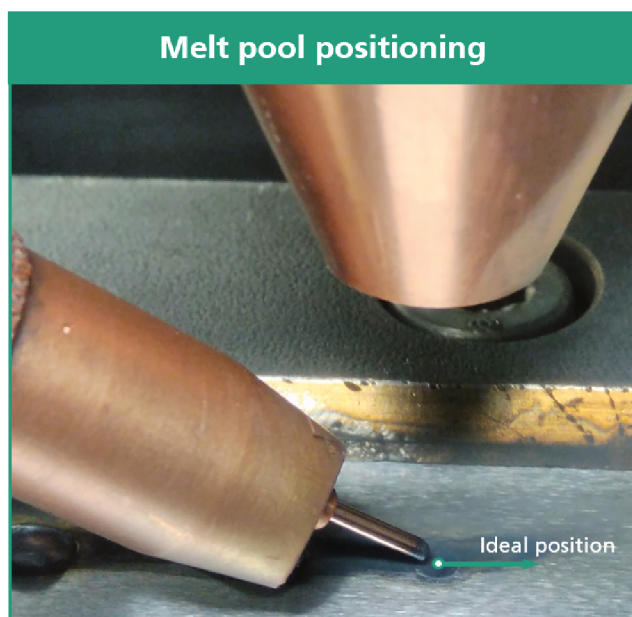
Comparing the results, the control that produced the best results in following the reference is in the Figure 49-C. The control Equation (37) used for this response is based on the first order model Equation (23). The z-force reaches its set point in less than one minute as designed.

The other control Equation (38) using the F_z also produced good results. However, as this control was designed in order to decrease the oscillation of the second order model, it takes more time until reaching its reference. Both response still have a small oscillation after reaching the setpoint.

From the Figure 49-A and -B, it can be observed that both depositions made using the resultant force as the process variable did not produce good responses. In reality, the response for the controls C_{res_1} and C_{res_2} are not stable. By looking at the step response from the identified model, this is not an expected outcome.

One reason can be used for explaining the difference in the capacity of the model when comparing to the data used for identifying the system and when applying this model to the control: The position of the wire in relation to the melt pool. This can be seen in the Figure 50.

Figure 50 – Melt Pool Positioning



Source: Original

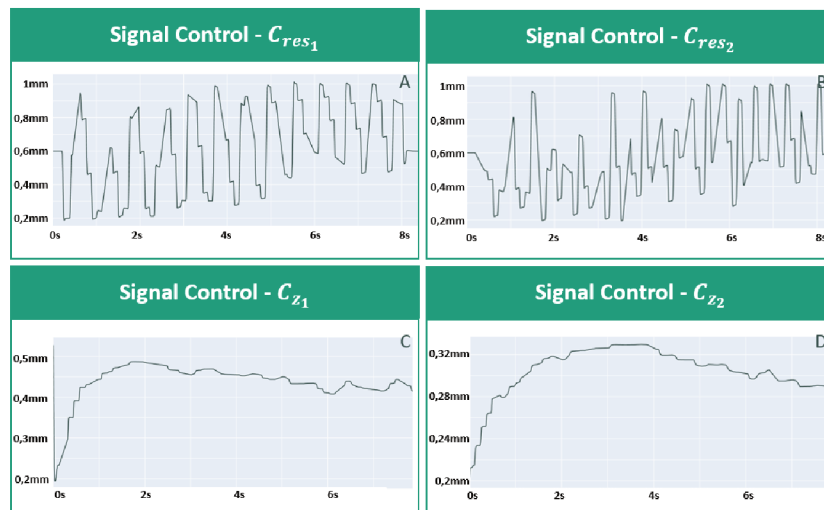
This difference between the wire position and the ideal position inside the melt pool needs to be correct regularly for a proper deposition. This reconfiguration can lead to different dynamics in the Y- and X- axis depending. As more than one axis affects this variable, it is more susceptible to these changes.

In the same way, a small difference on only one of these axis can lead to a

non-equivalent model. By observing this dynamic change, the best approach to this system is a time-variant model. In consequence, a real-time parameter identification is necessary. However, an online identification of the poles of the system is not studied in this project, as the objective of this project is finding a way of reaching a more stable deposition. In that way, the z-force response demonstrates a good solution.

Still using the second layer of the same deposition, in the Figure 51, a comparison between the control action from all the tests is demonstrated. Following the force response F_{res} setpoint, the control is unstable. This is observed in the Figure 51-A and -B.

Figure 51 – Comparison between the control action in the four tests



Source: Original

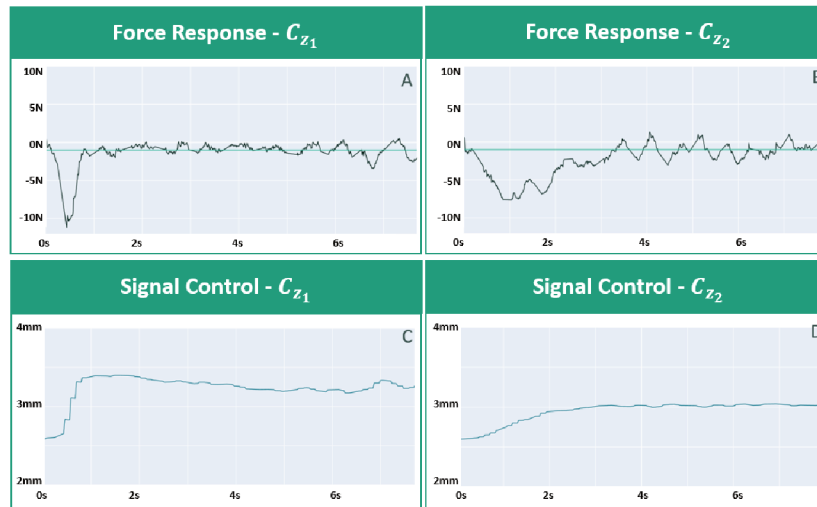
In the Figure 51-C and -D, the z force control can be observed. In contrast to the resultant force F_{res} , these control action does not have oscillations. As the process variable result, the second order control takes a longer time to accommodate. In fact, both control never reaches a steady value.

This can be explained by an existing angle in the substrate. As demonstrated in previous sections, this deviation can also be observed in the measured force. Thus, the control is acting to correct this difference. Another observed difference is the height of the tool. The control in the Figure 51-C is higher than the Figure 51-D.

This difference generates an offset in the next layer deposition. In the Figure 52, it can be observed a comparison between the two controls in the sixth layer of the same bead.

From the position tool, it can be observed that the first order control C_{z1} , seen in the Figure 52-C, still has a higher value than the second order control C_{z2} , seen in the Figure 52-D. For that reason, besides the initial force from the first bead is higher than

Figure 52 – Results for both Z-Control in the sixth layer



Source: Original

the second bead, the first reacts better.

By looking at Figure 52-A and -B, it is clear that the control C_{z1} produces a better response in aspect of reference following. Besides the bead already having five layers in the time of this deposition, the force response for this control still reaches a steady value of -1N in less than 1 second.

The setpoint of -1N for the z-force means that there is a traction between the wire feeder and the melt pool. By empirical evidence, when this measurement has positive values, the wire feeder is facing a resistance when applied to the melt pool. Depending on the amplitude of this resistance, the wire bend through the melt pool as demonstrated in the Figure 7.

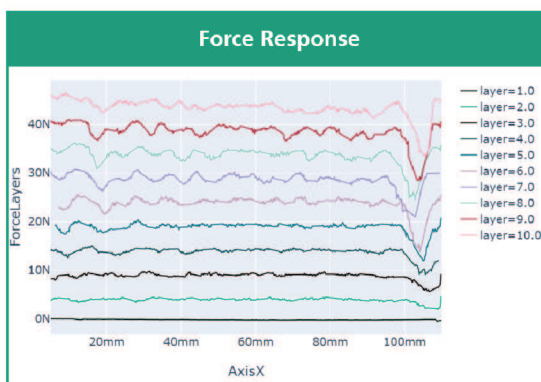
In contrast, the control C_{z2} also reaches the reference of -1N. However, this happens only at the middle of the deposition. In addition, the control action produces higher oscillations compared to the C_{z1} . By this analysis, it is evident the better response of the control C_{z1} .

At the end, an analysis from the result in all the layers of the control C_{z1} can be made. In the Figure 53, the forces during all the deposition in one bead is demonstrated. Each of this force has an offset of 5N for a better visualization.

A lot of conclusions can be obtained through this graph. First, the good reference following response between the second and five layer. The second layer has an approximate value of 4N. By defining the reference in -1N for all layers, this leads to a good reference following. In the Figure 53, a offset of 5N was added between each layer for a better visualization.

This can be observed until the fifth layer, where the reference is in 19N. However,

Figure 53 – Measured Forces in relation to the position in the deposition of all layers using the control C_{Z_1} with a default offset

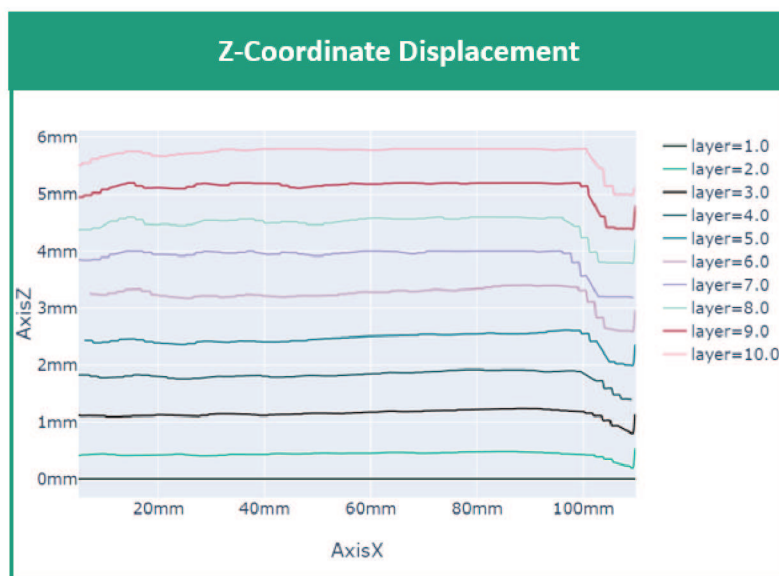


Source: Original

from the sixth layer is observed that the oscillation in the response starts to increase. Also, the peak in the force at the beginning of the deposition can be seen on the Figure 54. The deposition happens in the right direction, so the negative force can be seen in values higher than 100mm.

The setpoint of -1N was defined by empirical observation of good depositions in the first layers. By defining a good deposition, it can be concluded that the distance between the laser and the bead is in an ideal value, thus, the value of the force observed in these tests is selected for the setpoint of all the layers.

Figure 54 – Control action in the deposition of all layers using the Control C_{Z_1}



Source: Original

In the Figure 55, the source of this force can also be observed. Also, it is observed that after the control reaches its steady point, the resultant bead using the control exhibits a flat surface. From the Figure 53, it is observed at the end of the deposition how the error in one layer propagates to next.

In the sixth layer, a valley is observed at the end of the deposition. This valley is observed in the same place in all the following layers. The correction for this error can also be seen in the Figure 54. This demonstrates the importance of a control which produces no oscillation in the response. An oscillation can easily propagate to the next layer making the bead produced more unstable instead of improving its performance.

In the Figure 55, the bead produced with this control is observed. The different dynamics at the beginning can be seen on the right side of the bead. Also, it can be observed an inclination in the start of the deposition of the bead, where the control it is still not at the reference.

After that, the produced bead has the desired qualities of a laser metal deposition. It demonstrates a flat surface and a no-visible connection between each layer. This demonstrates the influence of this control in the final bead. Also, this establishes the potential of the controller in tracking the height offsets between layers and the inclination of a layer. This can be used in different control configurations and it is discussed in the next section.

Figure 55 – Resultant Bead using the control C_{Z_1}



Source: Original

6 CONCLUSION AND OUTLOOK

This document described the activities developed as part of the final project work for the automation and control engineering course from the University of Santa Catarina. This activity's goal is to provide the students an environment where they can put the knowledge acquired along the course in more practical real scenarios.

Almost all the automation and control engineering course's main areas have been used to deal with this problem. In the first place, the programming background obtained during the industrial informatics courses have been used to develop programs in different stages of this project.

The first stage of this work was creating a database for the future tests to be executed. For that purpose, a program was developed for acquiring, processing and sending the data to the MongoDB. This established database helped the continuity of this work and should be useful in next projects as a source of information in this process.

Nonetheless, this collection of data is not useful if there is no easy access for visualizing and studying it. Accordingly, a dashboard was developed providing the possibility of live monitoring the process status or retrieving data from a specific time. Also, a notebook jupyter for post processing the test data was also used along with the database.

For closing this process loop, the instrumentation theory acquired through the control and automation engineering course was used for communicating the FPGA with the CNC responsible for controlling the deposition tool.

Programming and Automation theory were used respectively to develop the labview program that sends the closing loop signal to the machine and to develop the G Cde that process this signal into the deposition. This was the first limitation faced during this work flow. The labview program would improve its performance if executed inside a better platform.

All these stages were successfully developed with the main goal of implementing a regulation in to the laser metal deposition with wire. Considering this objective, an important step was acquiring knowledge about the technique. As discussed during this document, a lot of factors can influence the final result of the LMD.

By studying these effects and getting familiar with the process, a better understanding of how to evaluate the produced beads and how to make its production more stable. Although evaluating the quality of the piece was not included in this project scope, this understanding helps to find a better tuning to the control.

From the obtained results in the control side of this project, the first analysis needs to be on the identification of the system. LMD-W has a complex dynamics and generalizing this into a single first or second order function certainly is not the ideal

solution.

This generalization must be used for evaluating the possibility of using the relationship of tool position offset and measured force to improve the performance of this technique. By considering this objective, the selected methods for identifying the system produced good results.

For investing in producing a model including the dynamics of more layers through step tests a better working environment needs to be prepared. This would require a greater control of variables outside this project for ensuring the reproducibility of the obtained data.

For example, all the layers must have the same temperature before the deposition to guarantee that this does not influence in the produced model. Nonetheless, the obtained result must also be motivation for following other alternatives to model the system and improve its performance.

A good control starts by reaching a good modeling of the system. Considering the generalization method used for identifying the system, the first assumption is that the control derived from it should produce good results but have certain limitations. The result analysis shows that all controllers have benefits and limitations while using it.

A good control is also finding the best balance on these benefits and limitations. As the results demonstrate, the regulations using z-force control have produced a good outcome in the first layers. Many arguments can be used for explaining this result, for example, the model was produced by doing tests in the first layers, so, its dynamics are well covered.

In the following layers, where the control was not able of correcting the accumulative errors, many actions can be taken. The performed analysis on the causes of the error accumulation is a first step on mitigating this problem. By studying these causes, it was possible to propose some alternatives to the control setup for decreasing its effect in the final bead.

Some of these alternatives showed promising results, however, they all require further tuning to reach their maximum effect. From the options to use as process variable, the resultant force produced sufficient results, but the better control was reached using the z-axis.

For the resultant force reaching a better result, an online identification of the poles of the system can be applied. By correcting the values of the system in real-time, the control can adapt for changes between layers due the different conditions, as temperature. Also, this approach corrects the different dynamics caused by the change in the wire feeder configuration.

For the z force, an online identification of the system also guarantees a better performance. As this variable is also susceptible for changes between layers, this can improve the performance in layers higher than six, where the system showed a decrease

in performance. As for this variable, the dynamics between beads showed a smaller deviation, this approach would result in an increase of the performance, however this improvement would not be as evident as for the resultant force.

A first step for this control is studying all the results saved in the database of this project. Also, future studies can follow other alternatives, such as, implementing a Multiple Input - Multiple Output (MIMO) system using all the force directions as the process variable. Then, the correction can be done in all three directions of the deposition tool. This can correct the problem of centrally feeding the wire into the melt pool.

In the height control aspect, it is possible also to use different parameters to implement a MIMO control. Studies using the laser power as control parameters have already been developed, as this variable directly affects the amount of wire deposited. Thus, this could be combined with the tool positioning for a future control.

In summary, this project reached a good result. The framework for acquiring, processing data and using it to control the system was well-implemented and a sufficient control was reached using it. Also, this opens the possibility of pursuing different solutions now that the system to implement it is already tested.

REFERENCES

ALMIR HERALIĆ; ANNA-KARIN CHRISTIANSSON; KJELL HURTIG, et al. Control Design for Automation of Robotized Laser Metal-wire Deposition. **IFAC Proceedings Volumes**, v. 41, n. 2, p. 14785–14791, 2008. ISSN 1474-6670. DOI: 10.3182/20080706-5-KR-1001.02503. Available from: <http://www.sciencedirect.com/science/article/pii/S1474667016413686>.

ALMIR HERALIĆ; ANNA-KARIN CHRISTIANSSON; MATTIAS OTTOSSON, et al. Increased stability in laser metal wire deposition through feedback from optical measurements. **Optics and Lasers in Engineering**, v. 48, n. 4, p. 478–485, 2010. ISSN 0143-8166. DOI: 10.1016/j.optlaseng.2009.08.012. Available from: <http://www.sciencedirect.com/science/article/pii/S0143816609002152>.

ASSOCIATION, Wohlers. **Wohlers Report**. [S.l.], 2018.

AUGUSTO RODRIGUES COELHO, ANTONIO AND DOS SANTOS COELHO, LEANDRO. Identificação de Sistemas Dinâmicos Lineares, 2016.

BRUECKNER, Frank et al. Process characteristics in high-precision laser metal deposition using wire and powder (Peer Reviewed). **Journal of Laser Applications**, v. 29, p. 022301, 2017. DOI: 10.2351/1.4983237.

COOPER, Kenneth G. Directed Energy Deposition Processes. In: RAPID Prototyping Technology. [S.l.]: CRC Press, 2001. ISBN 978-0824702618.

DING, Donghong et al. Wire-feed additive manufacturing of metal components: technologies, developments and future interests. **The International Journal of Advanced Manufacturing Technology**, v. 81, n. 1-4, p. 465–481, 2015. DOI: 10.1007/s00170-015-7077-3.

EDWARDS, Christopher; POSTLETHWAITE, Ian. Anti-windup and bumpless-transfer schemes. **Automatica**, v. 34, n. 2, p. 199–210, 1998. ISSN 0005-1098. DOI: [https://doi.org/10.1016/S0005-1098\(97\)00165-9](https://doi.org/10.1016/S0005-1098(97)00165-9). Available from: <http://www.sciencedirect.com/science/article/pii/S0005109897001659>.

FRAUNHOFER. [S.l.: s.n.], 2020. Available from: <https://www.ipt.fraunhofer.de/de/kontakt.html>.

GANTZ J, Reinsel D. Extracting value from chaos, p. 1112, 2011.

GAO, Wei et al. The status, challenges, and future of additive manufacturing in engineering. **Computer-Aided Design**, v. 69, p. 65–89, 2015. ISSN 00104485. DOI: 10.1016/j.cad.2015.04.001.

GEBHARDT, Andreas. **Generative Fertigungsverfahren: Additive Manufacturing und 3D Drucken für Prototyping ; Tooling ; Produktion**. 1. Aufl. s.l.: Carl Hanser Fachbuchverlag, 2013. ISBN 3446436510.

GEBLER, Malte; SCHOOT UITERKAMP, Anton J.M.; VISSER, Cindy. A global sustainability perspective on 3D printing technologies. **Energy Policy**, v. 74, p. 158–167, 2014. ISSN 03014215. DOI: 10.1016/j.enpol.2014.08.033.

GENE F., J. DAVID POWELL, ABBAS EMAMI-NAEINI. *Feedback Control of Dynamic*, 2010.

HAGQVIST, Petter; CHRISTIANSSON, Anna-Karin; HERALIC, Almir. Automation of a laser welding system for additive manufacturing. In: 2015 IEEE International Conference on Automation Science and Engineering (CASE). [S.l.]: IEEE, 2015. P. 900–905. DOI: 10.1109/CoASE.2015.7294213.

HAGQVIST, Petter; HERALIĆ, Almir, et al. Resistance based iterative learning control of additive manufacturing with wire. **Mechatronics**, v. 31, p. 116–123, 2015. ISSN 09574158. DOI: 10.1016/j.mechatronics.2015.03.008.

HAIRUL HISHAM HAMZAH et al. 3D printable conductive materials for the fabrication of electrochemical sensors: A mini review. **Electrochemistry Communications**, v. 96, p. 27–31, 2018. ISSN 1388-2481. DOI: 10.1016/j.elecom.2018.09.006. Available from: <http://www.sciencedirect.com/science/article/pii/S1388248118302212>.

J.T. HOFMAN et al. A camera based feedback control strategy for the laser cladding process. **Journal of Materials Processing Technology**, v. 212, n. 11, p. 2455–2462, 2012. ISSN 0924-0136. DOI: 10.1016/j.jmatprotec.2012.06.027. Available from: <http://www.sciencedirect.com/science/article/pii/S0924013612002063>.

K. LÖFFLER. 4 - Developments in disk laser welding. In: SEIJI KATAYAMA (Ed.). **Handbook of Laser Welding Technologies**. [S.l.]: Woodhead Publishing, 2013. (Woodhead Publishing Series in Electronic and Optical Materials). P. 73–102. ISBN 978-0-85709-264-9. DOI: 10.1533/9780857098771.1.73. Available from: <http://www.sciencedirect.com/science/article/pii/B9780857092649500040>.

KISTLER. **3-Component Force Sensor Fx, Fy, Fz Datasheet**. [S.l.: s.n.]. Available from: https://intertechnology.com/Kistler/pdfs/Force_Model_9067_9068_9066A4_9067A4.pdf.

LU, Bingheng; LI, Dichen; TIAN, Xiaoyong. Development Trends in Additive Manufacturing and 3D Printing. **Engineering**, v. 1, n. 1, p. 085–089, 2015. ISSN 20958099. DOI: 10.15302/J-ENG-2015012.

MAHAMOOD, Rasheedat et al. Laser Metal Deposition of Ti6Al4V: A Study on the Effect of Laser Power on Microstructure and Microhardness. **Lecture Notes in Engineering and Computer Science**, v. 2203, p. 994–999, 2013.

MATHWORKS. **MATLAB**. [S.l.: s.n.], 2017. Available from:
<https://www.mathworks.com/help/matlab/>.

NATIONAL INSTRUMENTS. **NI 9215 Datasheet**. [S.l.: s.n.], 2016. Available from:
http://www.ni.com/pdf/manuals/373779a_02.pdf.

NATIONAL INSTRUMENTS. **NI 9269 Datasheet**. [S.l.: s.n.], 2016. Available from:
http://www.ni.com/pdf/manuals/375099a_02.pdf.

NATIONAL INSTRUMENTS. **USER MANUAL AND SPECIFICATIONS NI cRIO-9075/9076**. [S.l.: s.n.]. Available from:
<https://www.ni.com/pdf/manuals/375650d.pdf>.

NATIONAL INSTRUMENTS CORPORATION. **LabVIEW: getting started with LabVIEW**. [S.l.: s.n.], 2013.

OGATA, Katsuhiko. **Modern control engineering**. [S.l.]: Pearson, 2016.

PRINTING)", "Charles Hull: Stereolithography (3D. National Inventors Hall of Fame, 2014.

SIEMENS. **SINUMERIK 840D sl / 828D Synchronized actions**. [S.l.: s.n.], 2012. Available from: https://support.industry.siemens.com/cs/attachments/64932968/FBSY_0712_en_en-US.pdf.

STEFAN KAIERLE et al. Review on Laser Deposition Welding: From Micro to Macro. **Physics Procedia**, v. 39, p. 336–345, 2012. ISSN 1875-3892. DOI: 10.1016/j.phpro.2012.10.046. Available from:
<http://www.sciencedirect.com/science/article/pii/S1875389212025734>.

TEAM, The Jupyter. **The Jupyter Notebook**. [S.l.: s.n.], 2019. Available from:
<https://jupyter-notebook.readthedocs.io/en/stable/notebook.html>.

WAHEED UL HAQ SYED; LIN LI. Effects of wire feeding direction and location in multiple layer diode laser direct metal deposition. **Applied Surface Science**, v. 248, n. 1, p. 518–524, 2005. ISSN 0169-4332. DOI: 10.1016/j.apsusc.2005.03.039. Available from:
<http://www.sciencedirect.com/science/article/pii/S0169433205004344>.

WONG, Kaufui V.; HERNANDEZ, Aldo. A Review of Additive Manufacturing. **ISRN Mechanical Engineering**, v. 2012, n. 4, p. 1–10, 2012. DOI: 10.5402/2012/208760.